



PERGAMON

Journal of Structural Geology 26 (2004) 537–557

**JOURNAL OF
STRUCTURAL
GEOLOGY**

www.elsevier.com/locate/jsg

Evolution of vertical faults at an extensional plate boundary, southwest Iceland

James V. Grant¹, Simon A. Kattenhorn*

Department of Geological Sciences, University of Idaho, PO Box 443022, Moscow, ID 83844-3022, USA

Received 15 August 2002; received in revised form 20 June 2003; accepted 24 July 2003

Abstract

Vertical faults having both opening and vertical displacements are common in southwest Iceland, and hypotheses vary regarding whether they propagated to the surface from below or from the surface downward. We address this issue through a study of vertical faults and associated surface fracture zones in regions of both oblique and normal spreading in southwest Iceland. Individual fracture segments are commonly rotated out of the general trend of the fracture zone, suggesting oblique motion along subsurface normal faults. These faults commonly breach the upper hinge lines of narrow monoclinial folds that flank many fault traces on the hanging wall side. Based on these field observations and the results of numerical models, we propose that 60–75° dipping normal faults in the subsurface propagated to the surface from below. Vertical fractures formed at the upper tips of the faults at depths of between 250 and 500 m (25–50% of the fault length) in response to stress concentrations along the tip line. Model results indicate that narrow monoclinial folds develop at the surface above these vertical fractures, which subsequently breach the monoclines along the upper hinge line, forming vertical fault scarps and open fissures at the surface. If vertical fractures utilize pre-existing cooling joints in basalt to connect directly to the surface, the hanging wall is able to pull apart from the footwall without the development of a surface monocline along the fault trace.

© 2003 Elsevier Ltd. All rights reserved.

Keywords: Iceland; Reykjanes; Spreading center; Normal fault; Vertical fault; Monocline

1. Introduction

Near-vertical scarps on surface-breaking normal faults have been documented in several areas around the world, including the rift zone in Iceland (Gudmundsson, 1980, 1987a,b, 1992; Opheim and Gudmundsson, 1989; Angelier et al., 1997), the East African Rift (Acocella et al., 2003), the Grabens area of Canyonlands National Park, Utah (McGill and Stromquist, 1975, 1979; Stromquist, 1976; Trudgill and Cartwright, 1994; Cartwright et al., 1995; Cartwright and Mansfield, 1998), the Koa'e fault system in Hawaii (Langley and Martel, 2000; Peacock and Parfitt, 2002), and the Hat Creek fault in northern California (Muffler et al., 1994). The combination of vertical and opening motions along vertical cracks implies that displacements are caused by slip along less steeply dipping normal fault planes at depth. However, whether these

normal faults (1) propagated to the surface from below, or (2) propagated from the surface downwards, is a contentious issue. This study provides arguments in support of the first explanation for vertical faults in southwest Iceland whereas previous Iceland studies typically promote the second explanation (Opheim and Gudmundsson, 1989; Gudmundsson, 1992).

Iceland is the only sub-aerial exposure of the extensional plate boundary between the Eurasian and North American plates. Several studies have addressed the origin of surface fracture swarms in southwest Iceland (Einarsson, 1967; Nakamura, 1970; Clifton, 2000; Clifton et al., 2000; Clifton and Schlische, 2003); however, those studies focused on the tectonic setting of the Reykjanes Peninsula, and not specifically the propagation direction or evolution of the normal faults themselves. Nonetheless, two of the studies (Einarsson, 1967; Nakamura, 1970) propose that subsurface faults may be responsible for the surface fracturing. For example, Einarsson (1967) interpreted the en échelon geometry of surface fractures and faults in postglacial lava in southwest Iceland as secondary fractures induced by

* Corresponding author. Tel.: +1-208-885-5063; fax: +1-208-885-5724.

E-mail address: simkat@uidaho.edu (S.A. Kattenhorn).

¹ Now at Anadarko Petroleum Corporation, Houston, TX, USA.

strike-slip motion on subsurface faults. In contrast, [Gudmundsson and Bäckström \(1991\)](#) and [Gudmundsson \(1992\)](#) specifically address the formation of normal faults in Iceland, suggesting that they either nucleated at the surface on large-scale tension fractures that propagated downwards to a critical depth of about 0.5 km, at which point they rotated into a typical normal fault dip, or they nucleated on sets of inclined columnar joints in tilted lava piles.

There are also conflicting hypotheses about the origin of vertical faults at the surface in regions outside of Iceland. [Acocella et al. \(2003\)](#) present a conceptual model for fault development in the Ethiopian Rift system that mirrors Iceland models of downward fault propagation. This growth pattern is suggested to cause the surface of the Earth to tilt away from the fault in the hanging wall. In the Grabens area of Canyonlands National Park, Utah, similarities to Icelandic faults have been invoked to hypothesize surface nucleation and downward propagation ([Cartwright et al., 1995](#); [Cartwright and Mansfield, 1998](#)). In contrast, upward propagation from below is favored by others ([McGill and Stromquist, 1975, 1979](#); [Stromquist, 1976](#)) using the reasoning that normal faults are not everywhere parallel to joint sets, they exist where jointing is not pervasive, and they have a systematic spacing. Upward propagation models

have also been proposed to explain the relationship between faulting and monoclinical folding at both the Koaie fault system on Kilauea Volcano in Hawaii ([Langley and Martel, 2000](#); [Peacock and Parfitt, 2002](#)), and in Quaternary and late Pliocene basalt lava flows at the Hat Creek fault in northern California ([Muffler et al., 1994](#)).

Despite these differing hypotheses regarding the propagation direction of normal faults, and despite the fact that the faults occur in different tectonic settings with varying rock types and loading conditions, they share many similar characteristics. At the surface the faults are all vertical, or near-vertical, have throw and opening displacements, and show no evidence of frictional contact between the fault surfaces. In each case, the surface portions of the vertical faults appear to have formed initially as tension fractures that subsequently accrued vertical displacement. Furthermore, vertical faults commonly have monoclinical flexures immediately adjacent to the fault scarp (e.g. Iceland, Koaie, and Hat Creek). The monoclines commonly extend beyond the lateral fault tips and exhibit tension fractures along the fold crests.

Fault growth models that propose fault initiation at the surface as tension fractures that then propagate to depth assume either explicitly ([Gudmundsson, 1992](#)) or implicitly

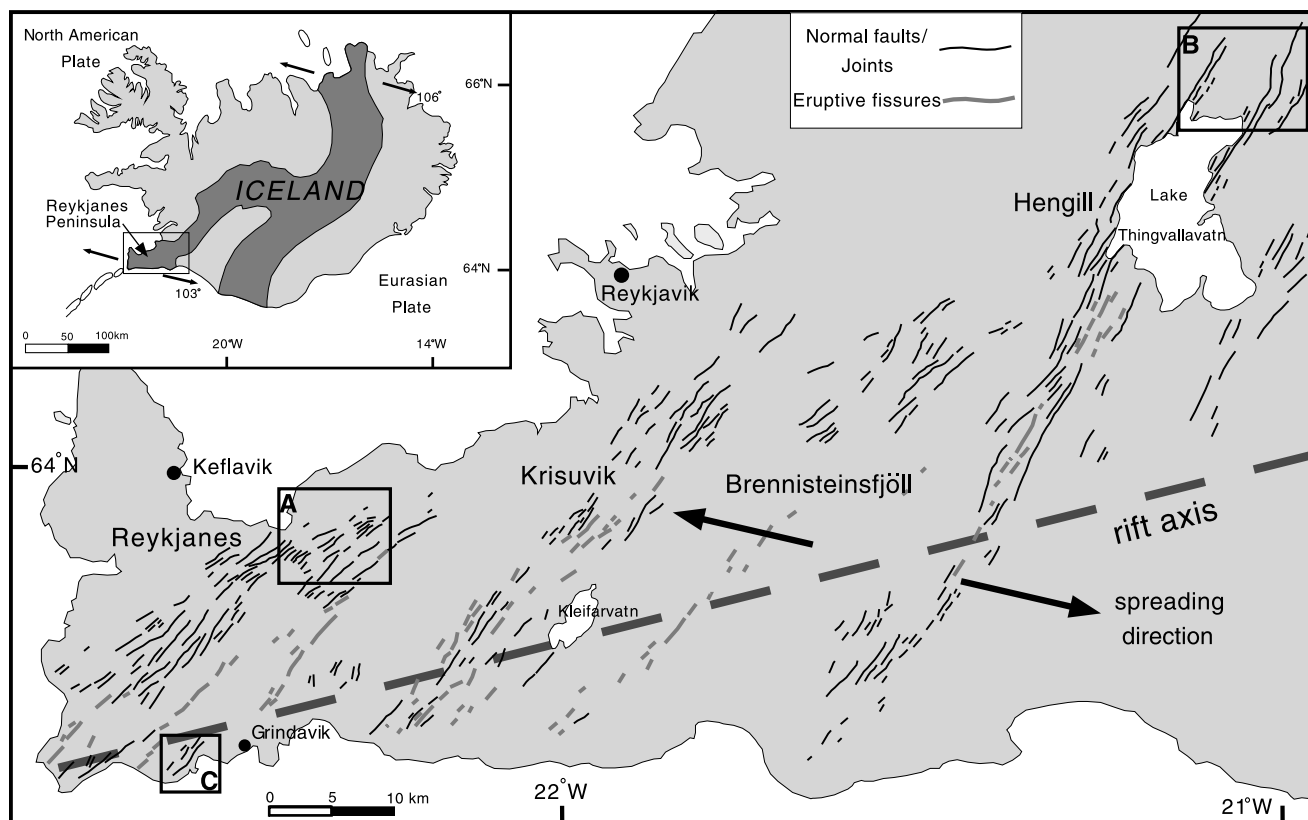


Fig. 1. Map of the Reykjanes Peninsula (box in inset map of Iceland) showing the locations of the four major fissure swarms. Black arrows show the direction of plate motions according to the NUVEL1-A model ([DeMets et al., 1994](#)), and the gray dashed line shows the approximate location of the rift axis. Dark gray shading in the inset map shows active volcanic zones. Boxes A, B, and C show the locations of the Vogar, Thingvellir, and Grindavik fissure swarms, respectively (modified after [Saemundsson and Einarsson, 1980](#)).

(Cartwright et al., 1995; Cartwright and Mansfield, 1998) that a regionally-distributed, absolute tensile stress at the surface was responsible for the initiation and downward propagation of the tension fractures. However, in situ stress measurements made in extensional tectonic environments (Haimson, 1979; Haimson and Rummel, 1982; Zoback and Healy, 1984; Stock et al., 1985) do not show a tendency for absolute tensile stresses to exist at or near the surface. Nonetheless, the fact remains that on the Reykjanes Peninsula in southwest Iceland, there exist at the surface both vertical tension fractures and vertical faults, the surface portions of which appear to have initiated as tension fractures. The occurrence of these structures implies absolute tension at the surface, but not necessarily on a regional scale.

The goal of this paper is to develop a mechanically-based, fault-evolution model that accounts for the development of vertical faults and observed surface deformation characteristics in southwest Iceland, and possibly elsewhere. We propose that the absolute tensile stresses responsible for the formation of vertical tension fractures are localized perturbations of the regional stress field caused by slip on subsurface normal faults that were propagating to the surface from below. This hypothesis is supported by linear-elastic, fracture-mechanics-based numerical models.

2. Geologic setting

2.1. Terminology

Fieldwork was concentrated in southwest Iceland, where the on-land portion of the Reykjanes Ridge spreading center is manifested by surface-breaking normal faults and other fracture types arranged into several fissure swarms (Fig. 1). The term ‘fissure swarm’ is used here as a non-specific reference to a group of normal faults, tension fractures, and eruptive volcanic fissures. We use the term ‘fault’ to describe any fracture across which there is > 1 m of vertical displacement. The faults described in this study are normal faults in the subsurface but are vertical faults at the surface having both dilational and vertical displacement components. We use the term ‘joint’ to describe any predominantly opening-mode fracture (tension fracture) that has < 1 m of vertical displacement. The term ‘fracture’ is used throughout to describe any relatively planar break in rock, characterized by two approximately parallel surfaces, with the relative displacement across the fracture being small relative to its length (Pollard and Aydin, 1988). Fractures typically change from a joint to a fault along the trace length. The Icelandic word *gjá* is used to identify these fractures in the fissure swarms (Williams, 1995) and appears in many of the official names of these features. The term ‘monocline’ is used to refer to single-limbed folds that flank fracture traces and typically have curved hinge zones. The locations of monoclinical folds are indicated in our fracture

maps by dashed lines that trace out the lower hinge of the fold, which was easily identifiable in the field. Arrows point down the slope of the fold limb.

2.2. Field locations

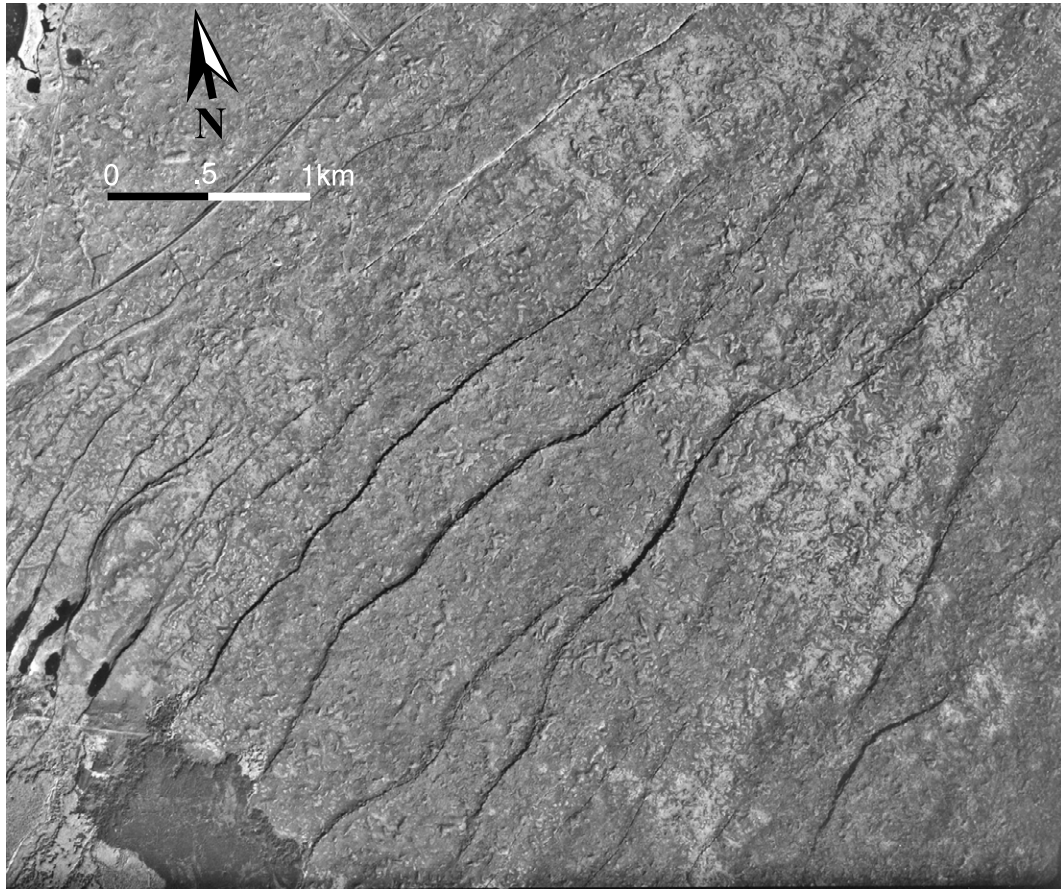
The Mid-Atlantic Ridge is an extensional plate boundary that crosses Iceland and separates the Eurasian plate from the North American plate. In Iceland, the plate boundary is defined by a series of seismic and volcanic rift zones (Fig. 1) (Einarsson, 1991). We chose two regions to examine vertical faults at the surface: the Reykjanes Peninsula, and the Thingvellir region, northeast of Reykjanes (Fig. 1). These sites were chosen in order to capture normal fault characteristics in regions of both oblique spreading (Reykjanes) and normal spreading (Thingvellir) to determine if a similar fault growth style could be identified.

On the Reykjanes Peninsula, the plate boundary (rift axis) is defined by a 2–5-km-wide zone of seismicity that trends $\sim 076^\circ$ (Vadon and Sigmundsson, 1997). The Reykjanes Peninsula is an obliquely-spreading ridge, with the plate boundary oriented $\sim 30^\circ$ oblique to the spreading direction (Fig. 1) (DeMets et al., 1994; Taylor et al., 1994; Clifton and Schlische, 2003). Four major fissure swarms occur in postglacial (younger than $\sim 12,000$ ybp) basaltic lava flows, each associated with a volcanic system (Gudmundsson, 1987a). Experimental models suggest that fault orientations are related to both the distance from the active rift axis and the obliquity of the extension direction with respect to the rift axis (Clifton et al., 2000). The trend of the rift axis at Thingvellir is $\sim 030^\circ$ (Gudmundsson, 1987b), approximately perpendicular to the plate spreading direction.

Normal faults, fault-related monoclines, joints, and eruptive fissures accommodate the regional extension at the surface. Both normal faults and joints utilize the pre-existing columnar joint network in the basalts at the surface, resulting in zigzag fracture traces. The overall trend of the fractures is governed by the local or regional extension direction. The fractures commonly exhibit significant apertures, some over 10 m in the Thingvellir area; however, present-day apertures do not necessarily represent the original tectonic apertures of the fractures due to collapse of blocks of basalt columns from the fracture walls. Our detailed fracture mapping for this study considered the Vogar and Grindavík regions on the obliquely-spreading Reykjanes Peninsula (box A and box C in Fig. 1), and the normal-spreading Thingvellir region (box B in Fig. 1).

Fracture trace maps of the three field areas were created from aerial photographs obtained from Landmælingar Íslands (Iceland Geodetic Survey). ERDAS Imagine software was used to spatially register and rectify the photographs with a geo-referenced digital road map. ArcView software was used to map fracture traces directly onto the aerial photographs. The fracture maps thus created were used to analyze the geometry of individual fracture

a.



b.

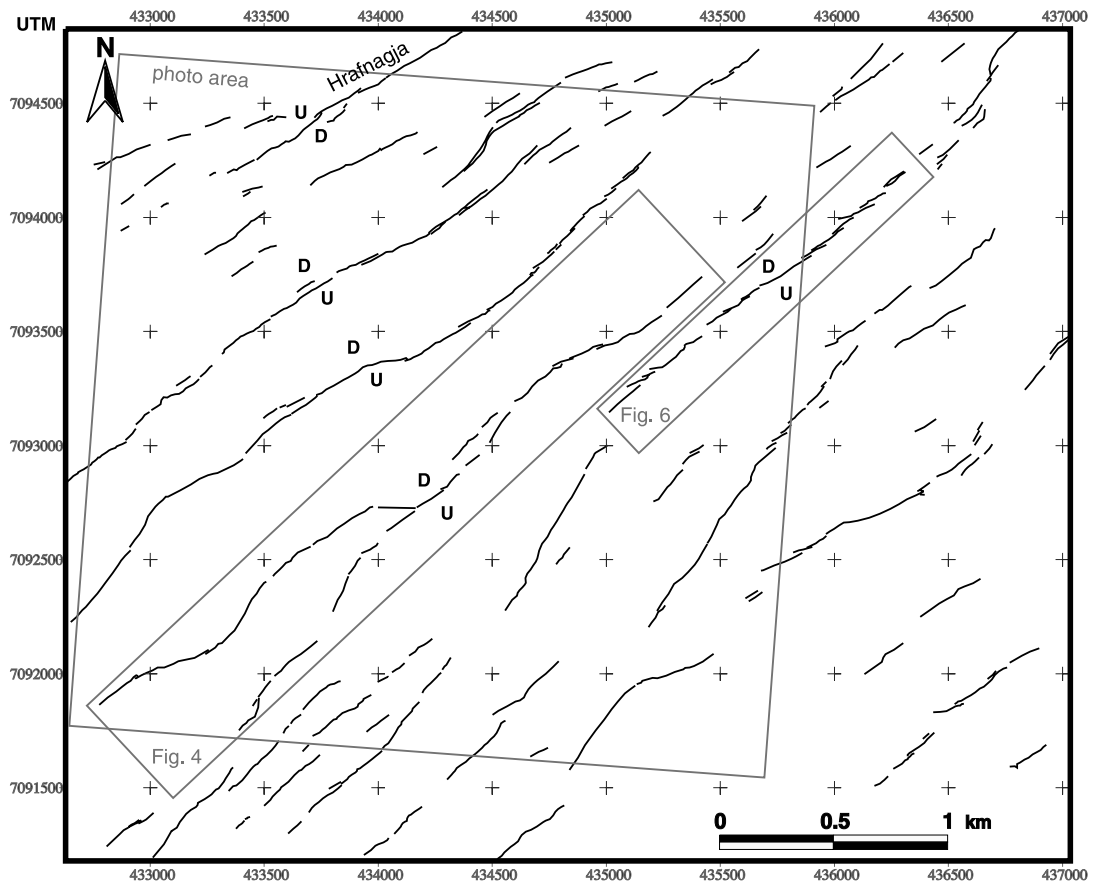




Fig. 3. Typical features along fracture zones in the Vogar fissure swarm. In this example, a surface monocline is breached by a fault along its upper hinge line. The fault displays both vertical and opening displacements and the fault scarp is vertical.

traces within each fissure swarm. Fractures within these fissure swarms have been previously mapped by other authors, and statistical analyses have been carried out on fracture length, width, throw and orientation data (Nakamura, 1970; Gudmundsson, 1980, 1987a,b; Clifton and Schlische, 2003). Nonetheless, our fracture trace maps are original so as to prevent undue influence by previous interpretations, and were used to identify specific locations within each area to investigate in detail in the field. UTM coordinates of the selected areas were recorded as waypoints in a handheld Global Positioning System in order to accurately locate specific field sites.

3. Field observations

3.1. Reykjanes Peninsula

3.1.1. Vogar

The Vogar fissure swarm is located at the northeastern end of the Reykjanes fissure swarm on the obliquely-spreading Reykjanes Peninsula, and dissects $\sim 7 \text{ km}^2$ of postglacial pahoehoe basaltic lavas erupted prior to 1100 ybp (Fig. 2) (Johannesson and Saemundsson, 1989). The surface deformation is characterized by near-vertical faults and joints, commonly flanked by narrow monoclinical folds (Fig. 3), all of which trend in a northeasterly direction. The down-dropped hanging walls of the normal faults are, in most cases, on the northwestern side of the faults, suggesting that in the subsurface they dip away from the rift axis towards the northwest. An exception is the fault

named Hrafnagjá, which defines the northern boundary of the Vogar fissure swarm.

Fracture traces that appear continuous in aerial photographs (Fig. 2) are actually highly segmented, regularly spaced, curvilinear zones of normal faults and joints, separated by regions of little or no fracturing (Fig. 2). Within each fracture zone, the fractures are arranged en échelon, such that individual fracture segments are rotated out of the general trend of the fracture zone. Left-stepping échelon arrangements predominate, with individual segments commonly linked together. The faults exhibit both vertical and opening components of displacement, resulting in gaping chasms along fault scarps that are open to depths of approximately 20 m down to rubble fill. No evidence of frictional contact of the fault surfaces was observed along any of the faults within the map area.

Beyond their lateral tips, the traces of normal faults continue as narrow monoclinical folds and/or linear clusters of tension fractures. Narrow monoclines also commonly flank the lengths of the fault traces on the hanging wall side (Fig. 3). Monocline hinge zones curve into relatively flat upper (footwall) and lower (hanging wall) extents. Fold limb dips range up to $\sim 30^\circ$ (Fig. 3). Where monoclines are not cut by faults, they typically exhibit clusters of parallel fractures that trace out the upper hinge lines of the monoclines. Such fractures exhibit little ($< 1 \text{ m}$) to no vertical offset.

The fractures in Fig. 4 (a portion of the Vogar fissure swarm that will be referred to as Simon's Gjá) were mapped from an aerial photograph at a scale of 1:23,000, complemented by detailed field mapping of the fracture traces. Simon's Gjá consists of two main fractures (Fracture 1 and Fracture 2) that are variably manifested along their trace lengths as either normal faults or joints associated with monoclinical flexures. Fracture 1 exhibits several scales of segmentation, with most individual segments having linked to form a through-going structure (Fig. 5). For example, Fracture 1 is segmented at the kilometer scale (Fig. 2), the 100 m scale (Fig. 4), and the meter scale (Fig. 4 inset). At all scales, segments display a left-stepping échelon arrangement.

Narrow monoclinical folds follow the trend of both fractures at Simon's Gjá. A monocline is present on the hanging wall side of Fracture 1 for a distance of approximately 1250 m from its southwestern end. Further to the northeast, a number of joints are located along the hanging wall of Fracture 1 where the monocline is absent. Fracture 2 consists of a narrow monoclinical fold cut by linear fracture segments that generally lack vertical displacement, except at its southwestern end. Beyond the southwestern end

Fig. 2. (a) Aerial photograph of part of the Vogar fissure swarm (box A in Fig. 1). Linear shadows indicate locations of normal faults, tension fractures, and monoclines (Photograph #M 0362, purchased from Landmælingar Íslands). (b) Fault and fracture trace map of the Vogar fissure swarm. Upthrown (U) and downthrown (D) sides of faults are as indicated. The large gray box shows the area covered by the aerial photograph in (a). Smaller gray boxes indicate the locations of detailed fracture maps shown in Figs. 4 and 6. Location grid is in UTM coordinates.

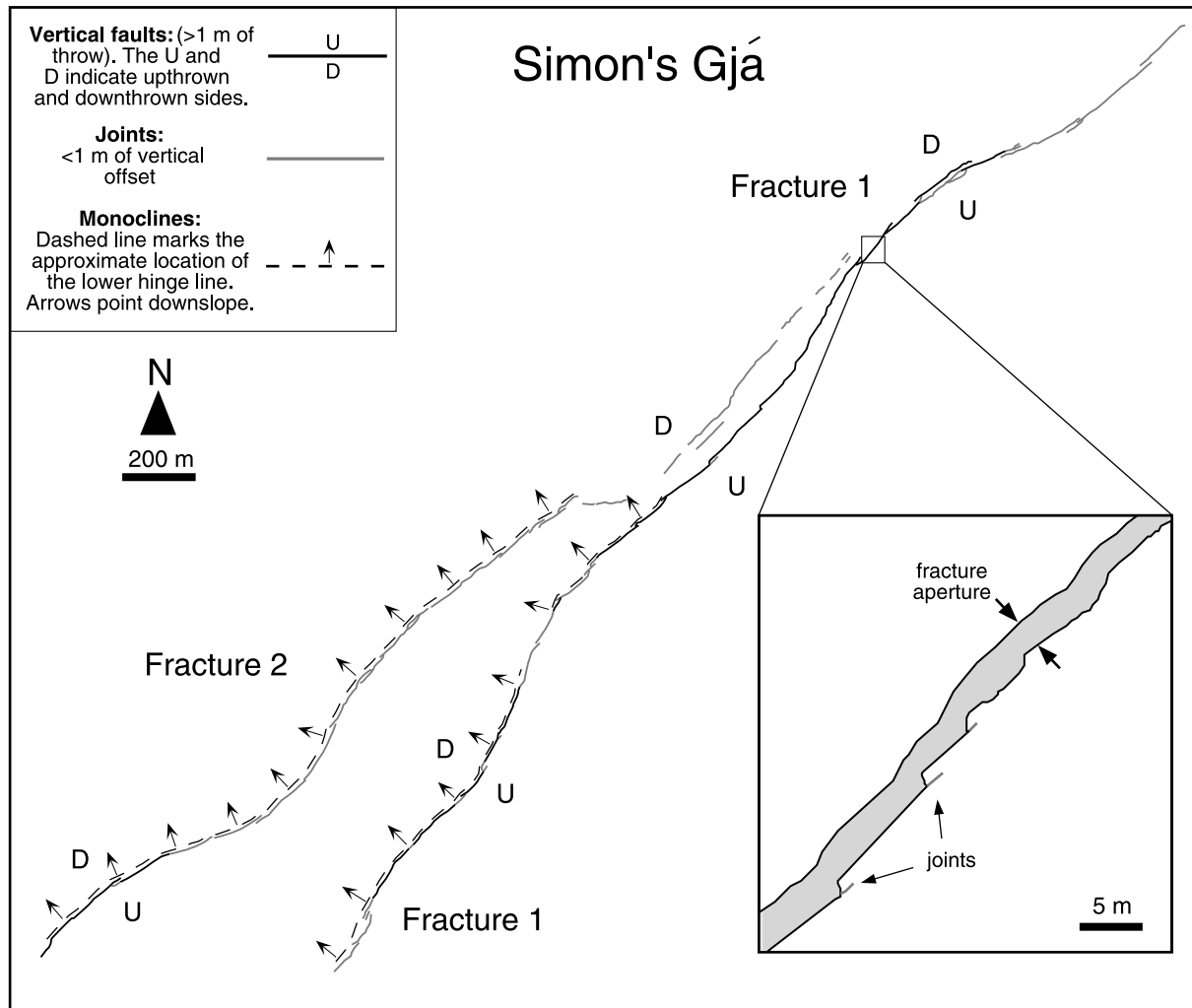


Fig. 4. Detailed fault and fracture map of Simon's Gjá in the Vogar fissure swarm (box in Fig. 2b). Both Fracture 1 (longer fracture) and Fracture 2 (adjacent, shorter fracture) are manifested variably along their traces as segmented vertical faults and open joints. A portion of Fracture 1 and all of Fracture 2 are flanked by hanging wall surface monoclines, shown as dashed lines with arrows pointing down the slope direction. Inset: meter-scale segmentation along a fault segment within Fracture 1. The segments have a left-stepping, échelon arrangement, and have linked together to form a through-going structure.

(Fig. 4), the fracture is covered by younger a'a basalt flows. The fractures are not arranged en échelon along the monocline, but consist of overlapping, parallel segments that trace out the upper hinge line (Fig. 4).

About 1 km northeast of Simon's Gjá, Echelon Gjá (Fig. 6) is comprised of a linear zone of left-stepping échelon fractures, accommodating 0–1.5 m of throw. The orientations of the individual fracture segments are plotted against the general trend of the fracture zone in the rose diagram in the lower right hand corner of Fig. 6, and differ by up to 30° from this trend. Where they accommodate throw, the fault segments are separated by relay ramps. Overlapping fault segments are typically hard-linked by joints that propagated from the tip of the segment on the footwall side of the overlap zone to intersect the segment on the hanging wall side. This is an upper ramp breach, using the terminology of Crider (2001), and resulted in a through-going normal fault.

3.1.2. Grindavík

The southeastern portion of the Reykjanes fissure swarm is located along the southern coast of the Reykjanes Peninsula. Clifton and Schlische (2003) refer to the general area as Grindavík (Fig. 7a), which lies on the southern fringe of the active rift zone. Vertical joints, normal faults, and monoclines characterize the deformation at the surface. The fractures are generally much shorter than those in the Vogar fissure swarm, and have accommodated significantly less throw (Clifton and Schlische, 2003). Nonetheless, the fracture zones at Grindavík (Fig. 7a) have very similar characteristics to the Vogar region (Fig. 2).

A 0.5-km-long normal fault was mapped just to the north of a golf course west of the town of Grindavík and is referred to here as Golf Course Gjá (Fig. 7b). The southeastern side of the fault has been down-dropped, implying that the fault dips to the southeast in the



Fig. 5. Left-stepping, échelon fault segments along Fracture 1 at Simon’s Gjá (view to the northeast). Each fault segment is rotated out of the overall trend of the fault zone. Total vertical offset is approximately 11 m. Note 1.9 m tall person in center of photograph for scale.

subsurface, away from the rift zone. Analogous to the Vogar region, the fault is comprised of a zone of left-stepping, commonly linked, échelon segments that are rotated out of the general trend of the fracture zone. A southeast-sloping monocline is located along the hanging wall side of the fault, and is breached by the fault along the upper hinge line.

3.2. Thingvellir

The Thingvellir fissure swarm is at the northeastern end of the Hengill fissure swarm, located to the northeast of the Hengill volcano on the north shore of Lake Thingvallavatn (Figs. 1 and 8). Unlike Vogar, this region is characterized by spreading normal to the rift zone. The fissure swarm is defined by a northeast–southwest oriented graben cutting a 9000-year-old pahoehoe lava flow (Gudmundsson, 1987b). Previous authors have calculated approximately 100 m of postglacial extension in the Thingvellir area; significantly more than the 15 m of postglacial extension calculated for Vogar (Gudmundsson, 1987b). The graben is bounded to the northwest by a 7.7-km-long, southeast-dipping normal fault named Almannagjá, and to the southeast by a 11-km-long, northeast-dipping normal fault named Hrafnagjá (Fig. 8), with maximum throw values of 28 and 14 m, respectively (Gudmundsson, 1987b). The three areas shown by boxes in Fig. 8 were field mapped to illustrate details of the fracture geometry.

The fracture map in Fig. 9 was created from the 1:6000 color aerial photograph of the main part of Thingvellir National Park located on the back of the 1:25,000 scale topographic map of Thingvellir (Landmælingar Íslands, 1994). The map illustrates the wide apertures of many of the fractures in this area (shown in gray), which are clustered into zones of numerous, approximately parallel, fractures. Almannagjá is a highly segmented normal fault that developed from the coalescence of numerous individual segments. Large slices of basalt mapped between the

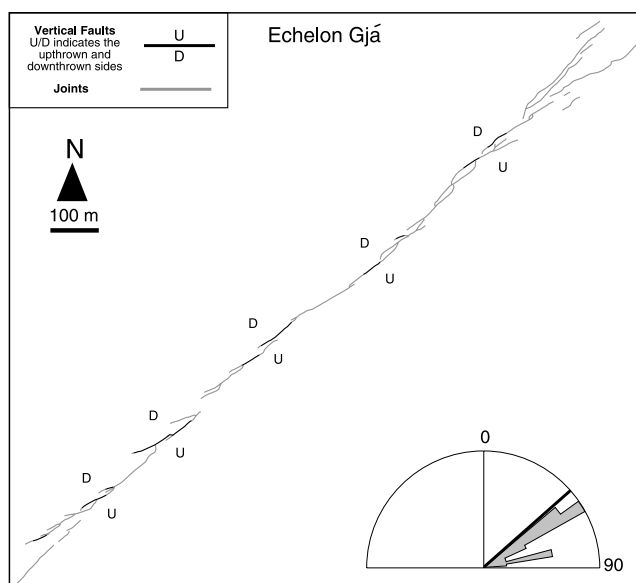


Fig. 6. Detailed fracture map of Echelon Gjá (box in Fig. 2b), illustrating a left-stepping, échelon arrangement of faults and joints. The trend of the individual fracture segments are plotted in gray in the rose diagram in the lower right, and the black line shows the general trend of the fracture zone.

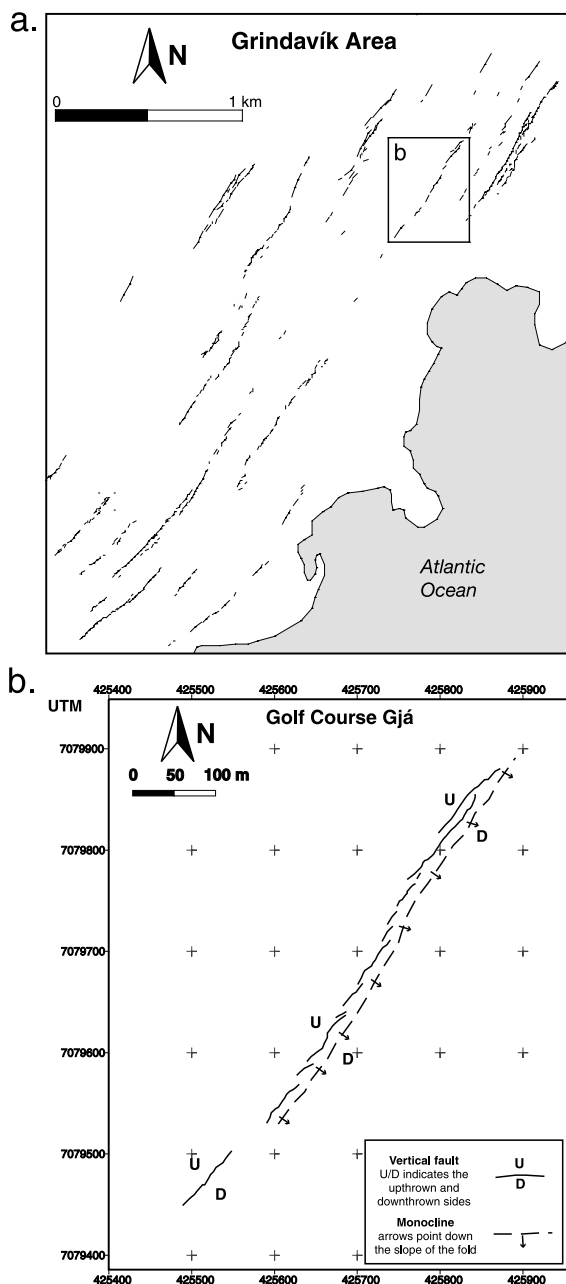


Fig. 7. (a) Fracture trace map of the Grindavík area (box C in Fig. 1). Box shows the location of the fracture map in (b) (after Clifton, 2000). (b) Left-stepping fault segments comprising Golf Course Gjá, with individual segments oriented at an angle to the general trend of the structure. A monocline flanks the fault trace on the hanging wall side. Location grid is in UTM coordinates.

bounding walls of the fault (Fig. 9) are remnants of the host rock between once unconnected, overlapping segments (Acocella et al., 2000). These slices can be observed in various stages of collapse along the trace of the fault. The hanging wall side of Almannagjá is associated with a large monocline, analogous to those observed at Vogar, although the Almannagjá monocline is 50–150 m wide, making it the largest fault-related monocline observed in this study (Fig. 10). We measured southeasterly dips

of the monocline ranging from 5 to 16°, although the dip may reach as high as 40° (Acocella, personal communication, 2003).

Several linear zones of joints and segmented normal faults occur to the southeast of the monocline (Fig. 9). The joints are arranged into discrete clusters, and have apertures of up to 20 m (Gudmundsson, 1987b). One normal fault in this area (Location 1 in Fig. 9) is comprised of a number of left-stepping échelon segments along a region of curvature in the overall fault trace. This fracture geometry differs from the fracture-zone-parallel arrangement of fractures in the more linear portions of the fracture zones at Thingvellir.

Figure 11a is a fracture map created from a 1:6600 scale aerial photo of the southern tip of Almannagjá, checked in the field for accuracy. The area consists of an ~021°-trending normal fault that curves to the southwest to an orientation of ~043° where it breaks down into a cluster of right-stepping échelon joints. The individual joints within the cluster are oriented from 028° to 041° where the general trend of the joint cluster along the fault bend is ~043° (see rose diagram in Fig. 11a inset). A southeast sloping monocline is present on the hanging wall side of the fault; however, it dies out towards the southwest along the fault bend where the fault trace is manifested solely by an échelon joint cluster.

Figure 11b is a fracture map of a portion of Gildruholtsgjá. The dense vegetation in this area makes it more difficult to see details of the fracture geometries in comparison to the fractures along the western side of Thingvellir graben. Where this fracture is mapped as a fault (solid black lines), there is <1 m of opening and Gudmundsson (1987b) measured up to 25 m of throw. Along the bend in the fault trace, the fault is comprised of a number of échelon segments, the arrangement of which changes from left- to right-stepping around the apex of the bend. Joints to the southwest of the fault bend accommodate 1–2 m of opening. Northeast of the fault bend, the fracture zone becomes more linear and is flanked by a monoclinical fold with a northwest dipping limb and with joints tracing out the upper hinge line.

4. Interpretation of field observations

4.1. Reykjanes Peninsula

Fractures in the Vogar fissure swarm occur either as zones of en échelon fractures or as clusters of parallel fractures that trace out the upper hinges of monoclines (Figs. 2–6). We interpret both types of fractures to be related to deformation above the upper tips of segmented, subsurface normal faults. We hypothesize that monoclines are the surface expression of subsurface normal faults, caused by flexure of the surface above upward-propagating fault tips. Fractures that breach the upper hinges of the monoclines are

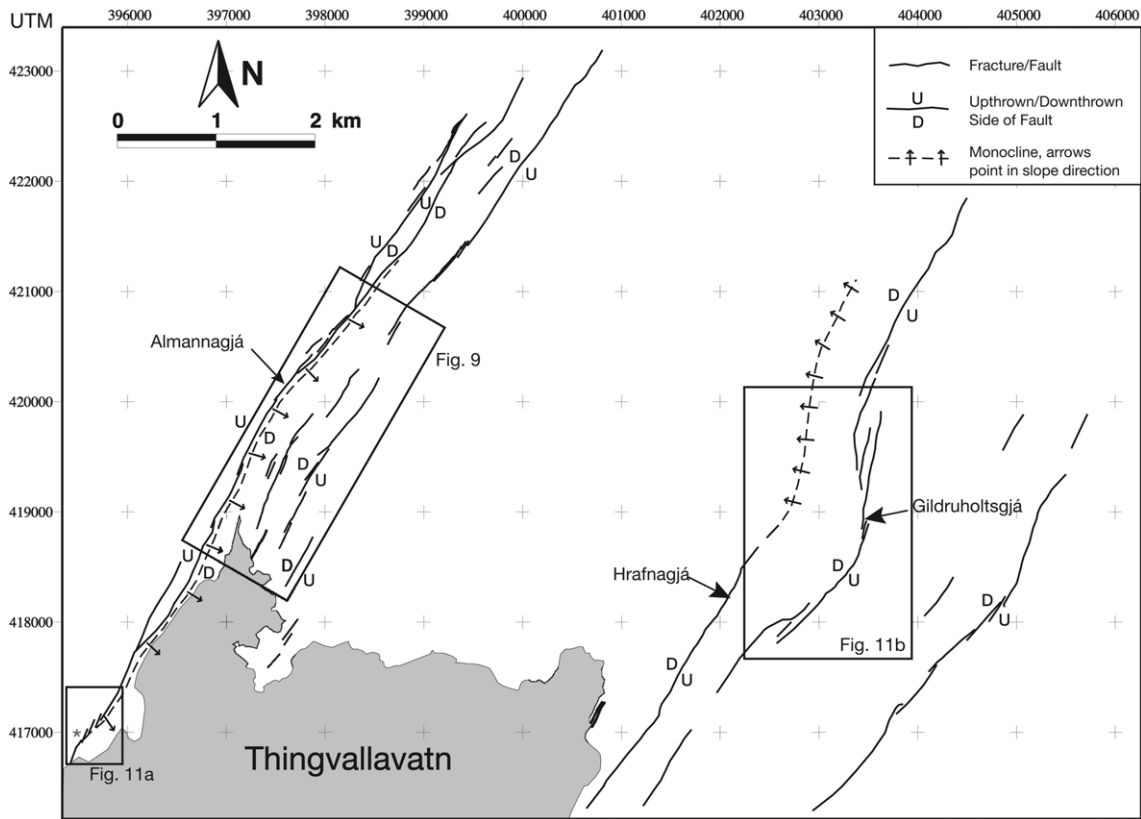


Fig. 8. Map of the Thingvellir fissure swarm (box B in Fig. 1), north of Lake Thingvallavatn, showing the orientations and locations of fractures, faults, and monoclines. Boxes show the locations of fracture maps in Figs. 9 and 11a and b. The star at the southern end of Almannagjá shows the location of the photograph in Fig. 10. Location grid is in UTM coordinates.

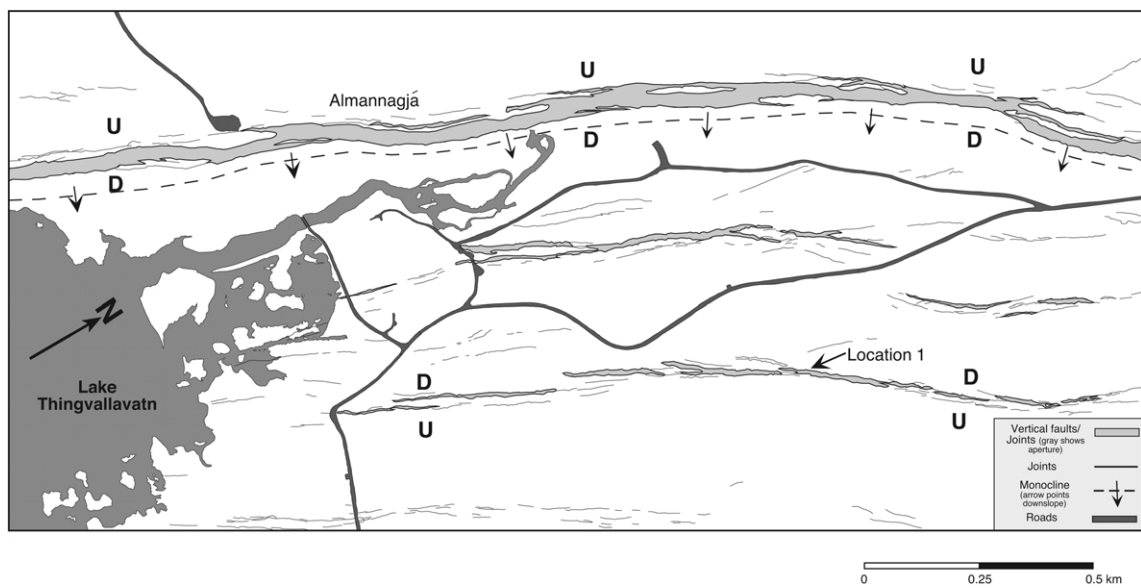


Fig. 9. Fracture map of vertical faults and joints in the Thingvellir fissure swarm (box in Fig. 8). Surface apertures are shown with light gray shading. The faults are segmented with individual segments oriented parallel to the overall trend of the fault trace except at bends in the faults, where en échelon patterns occur (Location 1 is referred to in the main text). Almannagjá is the most prominent fault and is associated with a hanging wall monocline that has been breached along its upper hinge line. Fracture zones in the hanging wall (southeast) of Almannagjá are antithetic to the main fault, which dips to the southeast in the subsurface.



Fig. 10. Surface monocline sloping towards Lake Thingvallavatn on the hanging wall side of Almannagjá in the Thingvellir fissure swarm (location of star in Fig. 8). View is towards the northeast. The upper hinge line of the monocline is breached by numerous right-stepping, échelon fractures. Note the summerhouses along the lakefront for scale.

semi-parallel to each other and to the trend of the monocline hinge (e.g. Fracture 2 in Fig. 4). This pattern of fracturing is consistent with bending-related tensile stresses in a monoclinical flexure.

We interpret fracture zones comprised of en échelon fractures (e.g. Fig. 6 and Fracture 1 in Fig. 4) to be the result of tensile stresses induced above the tips of obliquely-slipping subsurface faults. These fractures pierce the surface along a zone that parallels the trend of the underlying fault, with each individual fracture rotated out of the general trend of the fault. The combination of opening and throw displacements implies that the faults are not vertical in the subsurface but dip in the direction of the hanging wall block. Left-stepping, échelon fracture segments are common at Vogar, and are indicative of localized stress perturbations associated with right-lateral oblique slip along the upper tip line of a subsurface normal fault (Pollard et al., 1982; Schlische et al., 2002). Furthermore, the prevalent pattern of segment linkages, forming upper ramp breaches across relay zones, is consistent with right-lateral oblique slip along a left-stepping échelon fracture zone (Crider, 2001). Considering that normal faults form with strike orientations perpendicular to the least compressive principal stress direction, the right-lateral oblique slip motion suggested by the pattern of surface fracturing implies a clockwise rotation of the stress field between the time of initial normal fault growth at depth and the development of the surface fracture zones.

The fractures examined in the Grindavík area show characteristics similar to those seen in the Vogar fissure swarm; however, the longest fractures at Vogar are almost three times the length of those at Grindavík (Clifton and Schlische, 2003). The disparity in fracture lengths between the two areas is probably due to the scarcity of linked fracture segments at Grindavík in comparison to Vogar, suggesting that Grindavík is a less evolved analog of Vogar. The left-stepping échelon array of fractures that comprise Golf Course Gjá (Fig. 7b) are interpreted as having formed by right-lateral oblique motion along a subsurface fault, analogous to Vogar. These tension fractures subsequently propagated to the surface where they accommodated vertical displacements in response to ongoing slip on the underlying fault. The slip sense deduced for the subsurface fault suggests that, like at Vogar, there has been a clockwise rotation of the stress field between the initial formation of the normal fault and the development of the left-stepping segments exposed at the surface. Once again, we interpret the monoclinical fold on the hanging wall side of the fault (Fig. 7b) to indicate that the fault propagated to the surface from below.

4.2. Thingvellir

At Thingvellir, faults and joints are mostly semi-parallel to the trends of the fracture zones, reflecting an extension direction perpendicular to the rift zone. However, the

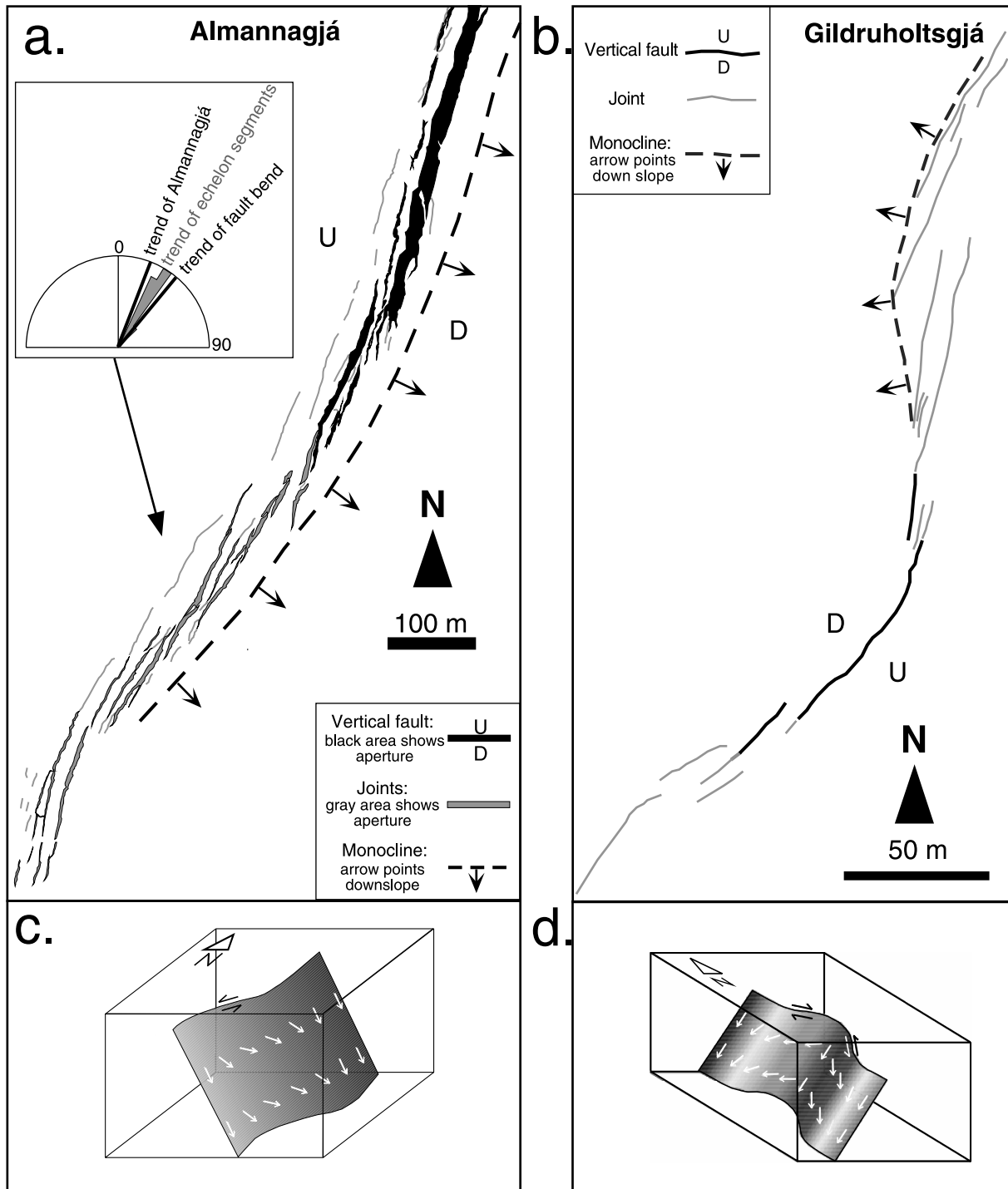


Fig. 11. Detailed fracture maps of the Thingvellir fissure swarm (boxes in Fig. 8). (a) Southwestern tip of Almannagjá where the fault trace bends along a right step, associated with a cluster of right-stepping échelon fractures. Fault (black) and joint (gray) apertures are shown for each fracture segment. The rose diagram (inset) shows the orientation of the individual joint segments along the bend in gray, as well as the general trend of Almannagjá both at and north of the fault bend. (b) Fault and joint segments that comprise Gildruholtsgjá, on the eastern side of Thingvellir. The fault trace is bent and fractures change from a right-stepping to a left-stepping arrangement around the apex of the bend. (c) Interpreted slip vectors on the underlying fault plane at the bend along Almannagjá, causing left-lateral oblique motion at the surface. Pure dip-slip motion occurs away from the fault bend. (d) Interpreted slip vectors on the underlying fault plane at the bend along Gildruholtsgjá, causing a transition (N to S) from right-lateral to left-lateral oblique motion at the surface around the apex of the fault bend. Pure dip-slip motion occurs away from the fault bend.

fracture zones are not perfectly linear and exhibit échelon fractures rotated out of the general trend of the fracture zone along bends in the fault traces (Fig. 11). This variability indicates that the échelon fractures did not form in the same stress field as along the linear portions of the fault zones but must instead represent localized perturbations of the stress field in the regions of fault bends. Along the linear portions of the fault zones, the fractures are parallel to the trend of the fault zone, consistent with dip-slip motion along a subsurface fault (e.g. Almannagjá; Fig. 9). This type of fault motion implies no rotation of the regional stress field between the time of formation of the subsurface normal faults and the development of the surface fracture clusters, unlike at Vogar.

We interpret en échelon segments at fault bends to be the result of localized oblique motion. The resultant échelon fractures are right-stepping where oblique motion includes a left-lateral component (Fig. 11a), and left-stepping where right-lateral oblique motion occurred (Fig. 11b). The bends in the fault traces at the surface imply an underlying pre-existing fault (Gudmundsson, 1987b), which we interpret to be the result of large-scale subsurface fault segment linkages between the more linear portions of the fault zones. Along Gildruholtsgjá (Fig. 11b), the transition from right- to left-stepping fractures occurs at the apex of a bend in the fault trace. Along linear portions of the fault trace, the fractures do not have an échelon arrangement. This fracture pattern is consistent with dip-slip motion along the underlying fault, with localized left-lateral oblique slip causing the right-stepping échelon fractures, and localized right-lateral oblique motion causing the left-stepping échelon fractures.

Similar to Vogar, monoclines occur along the hanging wall of many of the faults at Thingvellir such as Almannagjá (Fig. 10), Gildruholtsgjá (Fig. 11b), and Hrafnagjá (Fig. 8). The monoclines are all curved in map view, following the traces of the faults. If a segmented normal fault were to exist at some location in the subsurface and the segments were linked across the relay zone between them, the resultant fault trace would contain a bend, as is commonly seen along surface-breaking normal faults (dePolo et al., 1991; Machette et al., 1991; Zhang et al., 1991). If these linked fault segments were then to propagate up towards the surface, producing surface flexure above their upper tips, the resultant monocline should also be curved, as occurs at Thingvellir. This interpretation for the development of monoclines that are curved in map view is bolstered by the presence of échelon fractures along fault bends that imply control by an underlying fault undergoing oblique slip. Therefore, we interpret the surface deformation at Thingvellir to be consistent with upward propagating faults, analogous to Vogar and Grindavík on the Reykjanes Peninsula.

4.3. Summary of field interpretations

In all areas studied, fractures are arranged into discrete curvilinear zones, with little or no fracturing in the regions

between each fracture zone (Figs. 2 and 9). On the Reykjanes Peninsula, individual fracture segments are arranged en échelon, with the segments oriented at an angle to the general trend of fracture zones. At Thingvellir, fracture zones are mostly comprised of fractures that are parallel to the fracture zone trends; however, the zones are not perfectly linear and échelon fracture geometries occur along bends in the fracture zones. Previous hypotheses suggest that the Thingvellir fractures formed in response to a regionally distributed absolute tensile stress at the surface (Gudmundsson, 1992; Acocella et al., 2000). Wu and Pollard (1992, 1995) performed uniaxial tensile loading laboratory tests on thin brittle layers in order to describe the evolution of fractures in an absolute tensile stress field. Their experiments indicate that regional absolute tension at the surface results in parallel fractures with each segment oriented perpendicular to the maximum tensile stress. The distribution of these fractures is initially random, with no tendency for the formation of segmented fracture zones separated by regions of no fracturing. Numerical simulations of tensile fracture clustering (Renshaw and Pollard, 1994) produce a similar result. In none of these studies did fracture zones develop bends containing échelon fractures having different orientations to other fractures in the fracture zone. Based on these results, the fracture patterns that should develop in a region undergoing regional absolute tensile loading are inconsistent with the fracture patterns on the Reykjanes Peninsula and at Thingvellir.

Any model for fault development in southwest Iceland must also account for the presence of monoclinial folds alongside the faults. The monoclines are approximately 10–20 m wide, measured from the upper to lower hinge, at Vogar and Grindavík, and approximately 50–150 m wide along Almannagjá at Thingvellir. Monoclines accommodate the throw between the footwall and hanging wall blocks through a simple warping of the Earth's surface. Faults typically breach the monoclines at the surface along the upper hinge lines. It is unlikely that hanging wall monoclines developed alongside open, vertical fractures that had already pierced the Earth's surface because the vertical fractures would have acted as frictionless, shear-stress-free surfaces that effectively decoupled the footwall and hanging wall. The hanging wall could thus simply pull apart from the footwall without the need for monocline development to accommodate the throw. Using the same reasoning, if the faults initiated at the surface as tension fractures that subsequently propagated to depth and evolved into normal faults, monoclinial folding would not have occurred because the surface would already have been fractured when throw offsets began to accumulate.

These lines of reasoning for the development of fracture zones and monoclines in southwest Iceland leads us to conclude that both types of feature resulted from subsurface normal faults that propagated to the surface from below, contrasting with an existing model that advocates downward fault growth (e.g. Gudmundsson, 1992). Based on the

observation that faults are vertical at the surface, we hypothesize that as the faults propagated to the surface, vertical tension fractures formed above their upper tip lines at some critical depth. These tension fractures subsequently propagated to the surface in response to further slip on the fault. It is unclear from the field evidence whether the monoclines formed before or after the development of the vertical tension fractures above dipping faults. We examine this problem in the numerical modeling section (Section 5). The absence of flanking monoclines alongside some faults indicates that some vertical fractures were able to pierce the surface prior to the accumulation of throw along them. In such instances, tension fractures that developed above the upward propagating faults may have simply pulled apart pre-existing vertical cooling fractures in the columnar basalts, extending from the upper tip of the fault completely up to the surface, enabling the hanging wall to pull apart from the footwall during subsequent fault slip activity without the need for monocline development.

5. Numerical modeling

5.1. Motivation

Our field interpretations suggest that vertical faults in southwest Iceland propagated to the surface from below; however, a mechanical examination of the problem is needed to determine if such a model can account for the development of vertical fractures above subsurface faults, and if monoclines would be associated with upward fault growth. The development of extensional fault-related folds has been addressed previously using experimental models (Withjack et al., 1990), kinematic models (Erslev, 1991; Allmendinger, 1998), and numerical models (Patton and Fletcher, 1995; Willsey et al., 2002). The results of these studies show that slip on subsurface normal faults results in folding at the surface. Furthermore, experimental models (Schlische et al., 2002) and numerical models (Patton and Fletcher, 1995; Martel, 1997; Kattenhorn et al., 2000) suggest that joints can develop above the upper tip of a normal fault in response to high tensile stresses induced by fault slip. The joints that develop are predicted to be more steeply dipping than the fault plane, and subsequent slip events on the fault may cause the fault to propagate to the surface as a joint rather than a frictional fault. Joints are principal planes and so would be expected to intersect the shear-stress-free surface of the Earth at 90°, resulting in a vertical fault scarp like those observed in southwest Iceland.

There have been no comprehensive mechanical analyses of how slip on a subsurface normal fault with a joint along its upper tip line affects the displacement and stress field surrounding the fault. We use three-dimensional, linear-elastic fracture mechanics based numerical models to examine this problem. Specifically, we examine the effects of varying fault dip, depth below the surface, and the

addition of fractures of varying heights to the upper fault tip to determine how these parameters influence the surface displacements and near-fault stresses. Such models, referred to as forward models (e.g. Willsey et al., 2002), are not used to recreate nature explicitly but are nonetheless useful for gaining insights into the deformation field in response to variations in the physical configuration of the system. We conclude with a comparison between the model predictions and the characteristics of faults and monoclines observed in southwest Iceland.

5.2. Method

All numerical models were carried out using *Poly3D*: a three-dimensional, displacement discontinuity, boundary element computer program written by Thomas (1993). The program has been used in several previous studies of geological problems involving faulting (Willemse et al., 1996; Willemse, 1997; Crider and Pollard, 1998; Kattenhorn and Pollard, 1999, 2001; Kattenhorn et al., 2000; Maerten, 2000; Maerten et al., 2000, 2002; Crider, 2001). The program is based on the governing equations of linear elastic fracture mechanics for homogeneous and isotropic solids. In the models, faults are discretized into a number of triangular elements that act as planar dislocations of constant displacement discontinuity. The elements are combined to simulate a fault surface that is embedded in an elastic half-space. The surface of the half-space simulates the stress-free surface of the Earth. The faults are forced to slip in the models; however, due to the constraints of the numerical program, their dimensions are finite and the fault surfaces are not permitted to grow.

Slip on the faults is induced by applying shear stresses to each element on the fault, simulating the stress drop across the fault surface resolved from a tectonically-induced differential stress. Each element on the fault slips by an amount great enough to relieve the shear stress resolved onto it. The maximum slip occurs on the elements near to the center of the fault. Our analysis focuses on how slip on buried normal faults, with and without tension fractures along their upper tip line, perturbs the stress field surrounding them and causes displacements at the surface. This method allows us to isolate the fault-perturbed stress field very near to the fault and predict the types of secondary deformation that may result from these perturbations. The displacements in the elastic body containing the fault, including at the free surface, are governed by the stress drop and the amount of slip across the fault surface.

5.3. Model configuration

All the models simulate a 1-km-long by 1-km-high square fault discretized into 1600 triangular elements. Vertical fractures of varying heights in different models are connected to the upper tip line of the fault (Fig. 12). These fractures are discretized into triangular elements

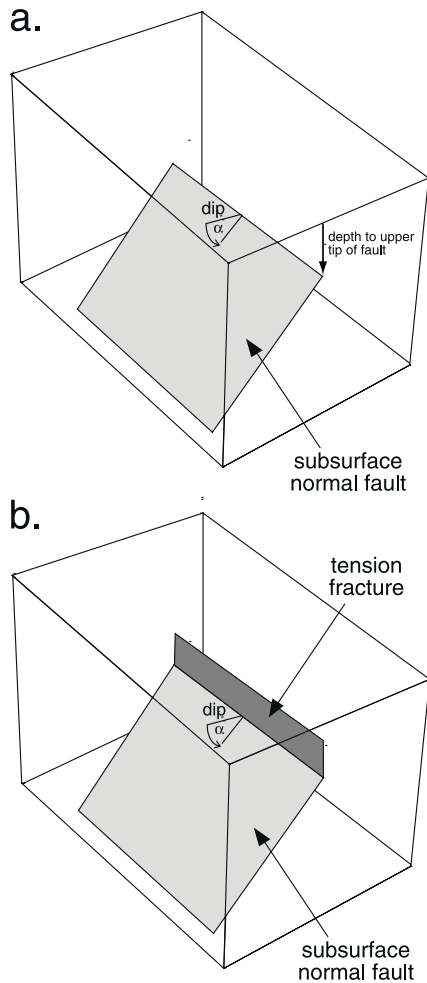


Fig. 12. Schematic drawing of the fault configuration used in the numerical models. (a) Subsurface normal fault with a square tip line, dipping at an angle α . (b) Subsurface normal fault with a vertical tension fracture along its upper tip line.

identically to the faults. Although normal faults in nature have been shown to have length-to-height aspect ratios > 1 in coal mines and three-dimensional seismic data (Walsh and Watterson, 1989; Mansfield and Cartwright, 1996; Nicol et al., 1996; Kattenhorn and Pollard, 2001), these aspect ratios may be the result of linkage of fault segments with initial aspect ratios closer to 1. Mechanical interaction between horizontally overlapping normal fault segments promotes lateral propagation of the segments which can result in composite faults with aspect ratios > 1 (Willemse, 1997; Kattenhorn and Pollard, 2001). By using square faults in our models, we make no assumptions about final fault

configurations that may result from linkages between such fault segments.

Three-dimensional seismic reflection images of normal faults show that the upper and lateral tip lines of normal faults are commonly approximately linear (Mansfield and Cartwright, 1996; Kattenhorn and Pollard, 2001), as in our models. A horizontal upper tip line may be expected if there is a critical depth at which fault shear failure gives way to tensile failure above the fault tip, or if the fault tip encounters a mechanical boundary that inhibits growth, such as at the contact between two lava flows. Sharp corners in the models influence both the displacements and the stresses in the area surrounding the fault corners; however, they are far enough away from our planes and lines of observation, where displacements and stresses are calculated, that their effect is miniscule.

The elastic properties of the material containing the faults are: Poisson's ratio $\nu = 0.25$, and elastic shear modulus, $G = 30$ GPa, which are reasonable values for basalt (Clark, 1966). Local boundary conditions applied to the faults in the models include a complete 1 MPa shear stress drop across the fault plane, and zero displacement constraint perpendicular to the fault surface so the fault surfaces remain in contact with each other. The walls of each vertical fracture are permitted to displace freely in response to slip on the underlying fault to which the fracture is connected.

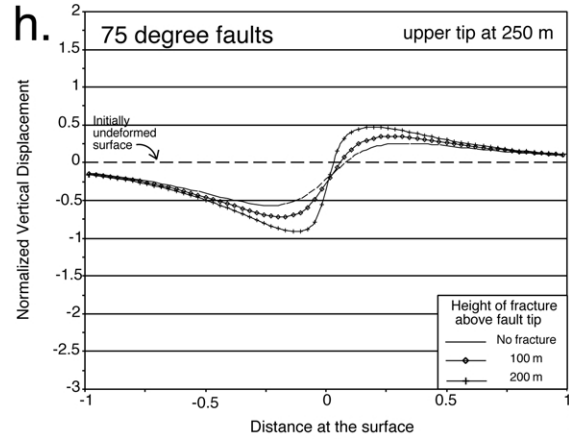
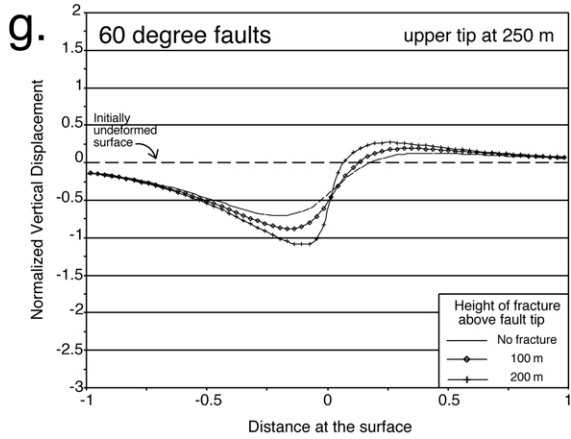
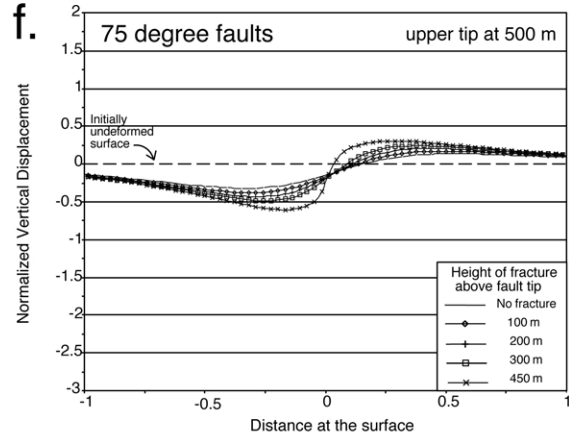
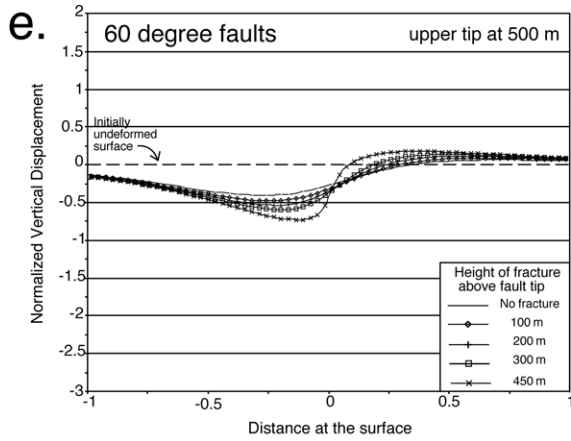
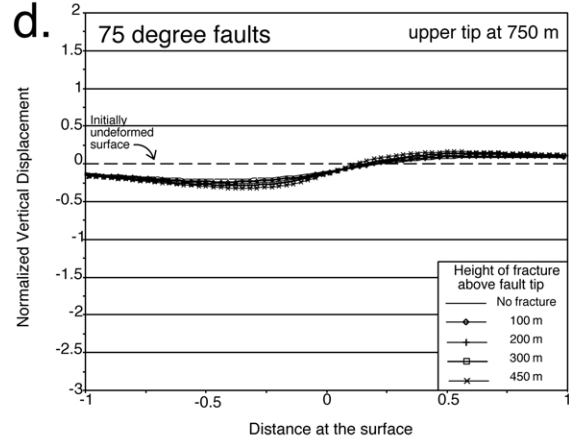
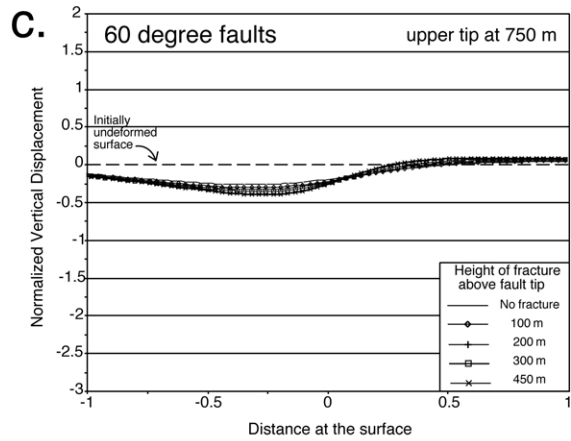
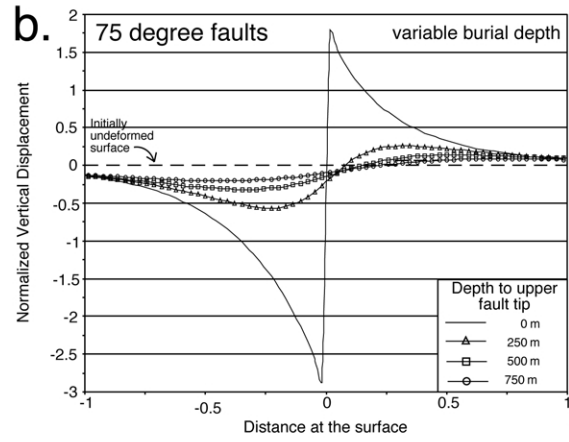
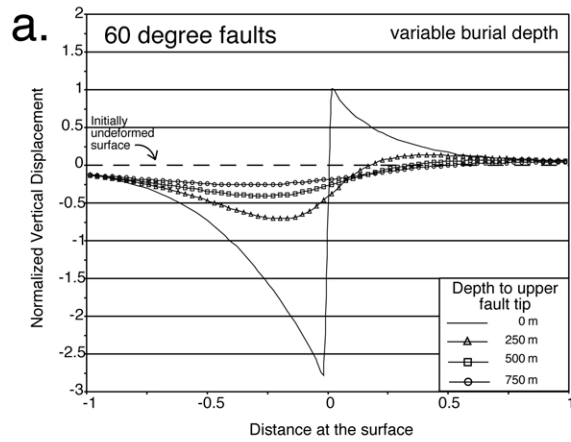
We examine the effect of varying the depth at which a dipping fault changes into a vertical fracture on resultant stress and displacement fields. At each fault depth, the height of the fracture along the upper tip line is varied to examine how fracture height affects the stress and displacement fields. These results are compared with the case of a dipping normal fault having no vertical fracture at its upper tip in order to demonstrate the importance of the vertical fracture for controlling the characteristics of the surface deformation.

5.4. Model results

5.4.1. Surface displacements

We examined the effect on surface displacements by subsurface normal faults dipping at 60° and 75° , respectively. Modeled faults were buried so that their upper tip lines were positioned at depths of 0, 250, 500, and 750 m below the surface of the half-space. At each of these depths (excluding 0 m), vertical fractures of varying heights were attached along the upper tip lines of the faults. Vertical displacements

Fig. 13. Vertical surface displacements along a line oriented perpendicular to the strike of a subsurface normal fault. In all cases, the fault dips to the left with its upper tip directly below the zero point on the 'distance at the surface' axis ($x = 0$). Horizontal distance away from this point is shown normalized to the fault length. Vertical displacements are normalized to the maximum uplift along a 60° dipping fault that pierces the earth's surface. The earth's surface is initially horizontal ($y = 0$). (a) and (b): 60° and 75° dipping normal faults, respectively, with the depth to the upper tip of the normal fault as indicated. (c) and (d): 60° and 75° dipping normal faults, respectively, with vertical fractures attached to a 750-m-deep normal fault upper tip. Fracture heights are as indicated. (e) and (f): Normal fault upper tips at 500 m depth with vertical fractures attached. (g) and (h): Normal fault upper tips at 250 m depth with vertical fractures attached.



at the surface are shown along a line perpendicular to fault strike above the fault centers (Fig. 13). For comparative purposes, the displacement values are normalized to the maximum footwall uplift induced at the surface by slip on a 60° fault that pierces the surface of the half-space. The horizontal dashed line at $y = 0$ shows the surface of the half-space prior to fault slip. Horizontal distance along the observation line is normalized to the fault length.

For the cases of 60° and 75° dipping normal faults having no vertical fractures attached, vertical surface displacements increase in both the footwall and hanging wall as the upper tip line more closely approaches the surface (Fig. 13a and b). There are no major differences in the patterns of displacements caused by the 15° difference in fault dip; however, 75° faults produce greater footwall uplift, and less hanging wall subsidence than 60° faults. With the exception of the case where the fault tip pierces the surface, slip on the faults results in broad monoclinial surface folding with steeper slopes above 75° faults. For buried faults, the maximum footwall uplift does not occur directly above where the fault tip projects vertically to the surface ($x = 0$), but further toward the footwall side of the fault.

Where subsurface faults have vertical fractures of varying heights attached to their upper tips, surface monoclines are narrower and more pronounced (Fig. 13c–h) than for faults having no fractures attached. The upper hinge lines of these monoclines are closer to the surface projection of the upper tip, but are nonetheless slightly toward the footwall side of the fault for both 60° and 75° faults. Surface folding appears to be less monoclinial and more like an anticline–syncline pair when vertical fractures approach within 50 m of the surface; however, this effect is exaggerated in Fig. 13 due to the vertical axis scaling. In actuality, the hanging wall curves gently upwards away from the base of the monocline fold limb over a distance approximately equivalent to the fault length, resulting in a surface slope of less than 1°. The surface displacement profile can thus be said to more closely resemble a monocline rather than an anticline–syncline pair.

Faults with their upper tip at 750 m depth (Fig. 13c and d) produce wide, low monoclines regardless of the fracture height at the upper tip. In contrast, faults with their upper tips at 250 and 500 m produce narrow monoclines above the surface projection of the fracture (Fig. 13e–h). Surface displacements progressively increase and the slope of the fold limb steepens as the vertical fracture increases in height and more closely approaches the free surface. Increasing fracture heights also cause the locations of the lower and upper fold hinges to migrate inward toward the surface projection of the fracture tip resulting in narrower folds, more so above 60° faults than above 75° faults.

5.4.2. Fault-perturbed stress field

Perturbed stress fields were examined around 60° faults buried with their upper tip lines at 250 and 500 m below the surface of the half-space (Fig. 14a and c). Horizontal distance perpendicular to fault strike is normalized to the

fault length. At each depth, we also examined the effect of a 200-m-high vertical fracture connected to the upper tip of the faults (Fig. 14b and d). Similar results were obtained for 75° faults; therefore, only the 60° fault case is shown. Boundary conditions were identical to those in the displacement models (Fig. 13). Maximum principal stress magnitudes (σ_1 , tension positive sign convention), normalized to the stress drop on the fault, were calculated on a plane through the fault center, oriented perpendicular to fault strike (Fig. 14). Hachured zones represent compressive stresses. The plane covers the upper half of the fault and extends to the surface of the half-space. These stresses represent the perturbed component of the total stress field in the elastic body containing the fault, induced by the slip event.

At both fault depths that were modeled (Fig. 14a and c), a region of high tensile stresses occurs above the upper tips of the faults, with the highest stresses occurring directly above the fault tip. The stress field at the surface is virtually unaffected for the case where the upper tip is at 500 m depth. For faults with their upper tip at 250 m, an area of increased tension occurs at the surface in the footwall, with lobes of compression underneath, below the fault tip.

The addition of 200-m-high fractures to each fault alters the perturbed stress field around the faults (Fig. 14b and d). In each case, zones of increased tension occur in the hanging wall, with the greatest tension occurring at the upper tip of the vertical fracture. This region of increased tension extends above the vertical fracture into the footwall at the surface. The absolute magnitude of the stresses for the 500-m-deep faults are much lower at the surface than they are for the 250-m-deep faults, which produce surface tension closer to the surface projection of the vertical fracture than for 500-m-deep faults.

6. Discussion

Although previous work conventionally proposes a downward growth model for normal faults in Iceland (Opheim and Gudmundsson, 1989; Gudmundsson, 1992), our field observations and model results in southwest Iceland lead us to propose an alternative hypothesis for normal fault growth involving propagation of faults to the surface from below. This hypothesis is predicated on: (1) the occurrence of discrete fracture zones containing échelon fractures where spreading is oblique, as well as along bends in fault traces where spreading is normal; and (2) the common association of fracture zones with flanking narrow monoclines.

Échelon fractures arranged into linear zones oriented oblique to the spreading direction on the Reykjanes Peninsula (Figs. 2, 4, 6 and 7) are interpreted to have formed above the tips of obliquely-slipping, subsurface faults. At Thingvellir, where plate spreading is perpendicular to the fracture zones, fractures are typically parallel to the fracture zones except at bends in the fault traces, where

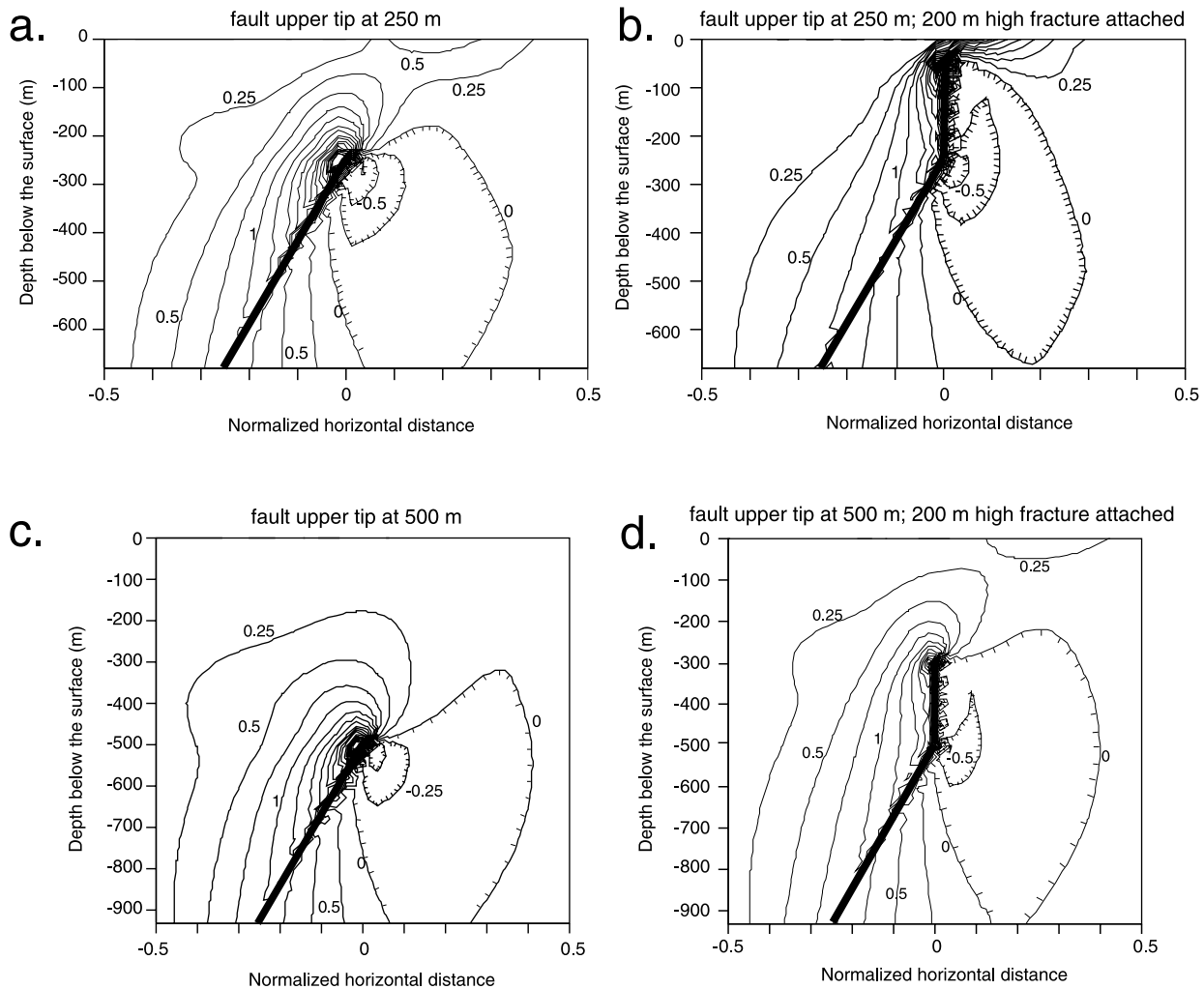


Fig. 14. Fault-perturbed stress fields contoured on a cross-section through the top of 60° dipping normal faults. The contours show the maximum principal stress magnitude (tension is positive) normalized to the stress drop across the fault surface. Hachured contours indicate zones of compression. Horizontal distance perpendicular to fault strike is normalized to fault length. (a) Fault tip at a depth of 250 m. A zone of tension extends from the fault tip to the surface. (b) As with (a) but with a 200-m-high vertical fracture attached to the fault tip. Surface tension occurs on the footwall side of the fault. (c) Fault tip at 500 m depth. (d) As with (c) but with a 200-m-high fracture attached to the fault. A zone of surface tension occurs on the footwall side of the fault.

échelon fractures occur (Figs. 9–11). This pattern of fractures is consistent with having formed above subsurface dip-slip faults where the fault trace is linear, with local oblique-slip along subsurface fault segment linkage sites, manifested at the surface as bends in the fault traces and associated échelon fracturing (Fig. 11).

The presence of monoclinical folds flanking normal faults bolsters this model of upward fault growth. Our reasoning is that surface folding is necessary to accommodate throw along an underlying fault in instances where the hanging wall and footwall are not decoupled at the surface by a vertical fracture, in which case the two sides of the fault are unable to simply pull apart from each other at the surface. If faults began growing at the surface as vertical tension fractures then the hanging wall and footwall would always be decoupled at the surface and no surface folding would be needed to accommodate surface throw.

The occurrence of monoclinical folding alongside surface breaking normal faults has been documented in several other locations around the world (Muffler et al., 1994; Langley and Martel, 2000; Peacock and Parfitt, 2002; Willsey et al., 2002) where the faults are believed to have propagated to the surface from depth. Experimental models (Withjack et al., 1990), kinematic models (Erslev, 1991; Allmendinger, 1998), and mechanical models (Willsey et al., 2002) all demonstrate that monoclinical folds can form above subsurface normal faults, with more steeply dipping faults producing narrower monoclines at the surface. Steeply dipping fractures can develop above the upper tips of the faults and propagate to the surface, breaching the monocline (Withjack et al., 1990). The results of these studies are all compatible with our interpretation that the fault-related monoclines in southwest Iceland developed above upward-propagating normal faults; however, they do not address

how the formation of a vertical fracture at the upper fault tip of a subsurface fault alters the geometry of the folding at the surface.

The model results presented in this study demonstrate that the geometry of surface folding is greatly affected by the addition of a vertical fracture along the upper tip line of the underlying fault. Slip on buried faults without fractures along their upper tip line result in the formation of gently sloping monoclines at the surface, several kilometers wide (Fig. 13a and b). This monocline geometry is inconsistent with field observations in southwest Iceland. However, high tensile stresses at the upper fault tip (Fig. 14) are of great enough magnitude to overcome the lithostatic compression and the tensile strength of the rock, which may have resulted in the growth of a vertical fracture above the fault tip. Our model results show that for faults buried no deeper than 500 m (or 50% of the fault length), the addition of a vertical fracture to the upper fault tip causes the zone of folding to become very narrow (up to a few hundred meters wide), with the upper and lower fold hinges progressively migrating towards each other as the fracture height increases (Fig. 13e–h). This model result is consistent with the narrow monoclines observed in the field, suggesting that the natural monoclines developed above dipping faults with vertical fractures at their upper tips rather than above faults having no vertical fractures.

Very narrow folds (<200 m wide), like those observed in the field, are not produced until the upper tip of the vertical fracture is at least 50 m below the surface for faults with their upper tips at 250 and 500 m (Fig. 13e–h). Model results for the 250-m-deep fault show synclinal troughs on the hanging wall side of the fault (vertically exaggerated in Fig. 13g and h); however, the actual slope of the hanging wall surface away from the fault trace is less than 1°, which would appear to be a horizontal basalt surface in the field. The displacement profile above the 500-m-deep fault with a 450 m vertical fracture at its upper tip (Fig. 13e and f) shows even shallower surface slopes than the 250-m-deep fault, thus more closely approximating a monoclinical profile. In comparison, the monocline at Thingvellir has a flat top (Fig. 10; compare with Fig. 13e and f) and an approximately flat bottom that slopes gently upwards over a distance of several kilometers away from the fault, as seen in the 1:25,000 scale topographic map of Thingvellir (Landmælingar Íslands, 1994). The results of all the models constrain upper fault tip depths to between 250 and 500 m (25–50% of the fault length). The height of the vertical fractures is thus several hundred meters at the instant that they breach the surface. This value is consistent with previous estimates based on fracture zone spacing at Vogar and Thingvellir (Gudmundsson, 1987a,b).

It is important to realize that the vertical displacements produced in our models represent the effect of a single slip event on a subsurface normal fault. Prior to this slip event, the surface of the half-space is perfectly planar. In reality, as the fault and/or fracture above the fault tip propagates

towards the surface, each slip event results in displacements at the surface, and the displacements from each event superimpose each other. Our models cannot account for this superimposition of displacements, which would be different for each fault, nor do we consider the potential effects of flexural slip along lava flow boundaries during the folding. Nonetheless, the model results elucidate the general pattern of surface displacements above normal faults with vertical fractures of varying height at their upper tips and thus provide some constraint on the subsurface geometry of the faults in southwest Iceland.

Another important consideration in the models is that the vertical fracture is not permitted to grow during the fault slip event. Folding thus occurs above a fracture of fixed height. This constraint may occur in nature if fracture growth is inhibited by a mechanical boundary such as a lava flow boundary or a sedimentary interbed. However, if a vertical fracture forms above a fault tip and instantly connects to the surface by utilizing the network of pre-existing cooling fractures in the basalt, the hanging wall can pull apart from the footwall without a monocline forming, as occurs along many fault zones in southwest Iceland (Figs. 4–6).

Although our model results simulate monocline development above vertical fractures reasonably well, we must still reconcile the model predictions of an upper monoclinical hinge on the footwall side of the vertical fracture with field observations of surface breakage through the upper hinge, leaving the monocline on the hanging wall side of the fault trace. The upward projection of the vertical fracture in the models bisects the monocline limb; however, a zone of increased tension is predicted to occur at the surface in the models (Fig. 14c and d), corresponding to the approximate location of the upper hinge of the monocline in the footwall. This zone of increased tension connects to the upper tip of the fracture in the subsurface (Fig. 14b and d). The implication is that a fracture propagating upwards from the upper tip of a fault would curve towards the footwall and breach the surface along the upper hinge of the monocline, leaving the monocline on the hanging wall side of the fault trace, consistent with our field observations (e.g. Simon's Gjá in Fig. 4). Once a fracture breaches the surface, subsequent slip events would result in vertical and opening displacements along the vertical scarp at the surface.

Bending stresses along the monocline upper hinge may augment the likelihood of surface breakage at this location, resulting in fracturing parallel to the hinge line (e.g. Fracture 2 in Fig. 4). In some cases, monocline hinges are breached by échelon fault segments rotated out of the trend of the monocline hinge line (e.g. Golf Course Gjá in Fig. 7b and Almannagjá in Figs. 10 and 11). The presence of a narrow monocline suggests that the upper tip of the vertical fracture was close to the surface. Oblique motion along the vertical fracture and the underlying fault at this point in the fault evolution (e.g. due to a rotation of the regional stress field at Golf Course Gjá or along a fault bend at Almannagjá) would have resulted in a rotation of the principal stresses above the

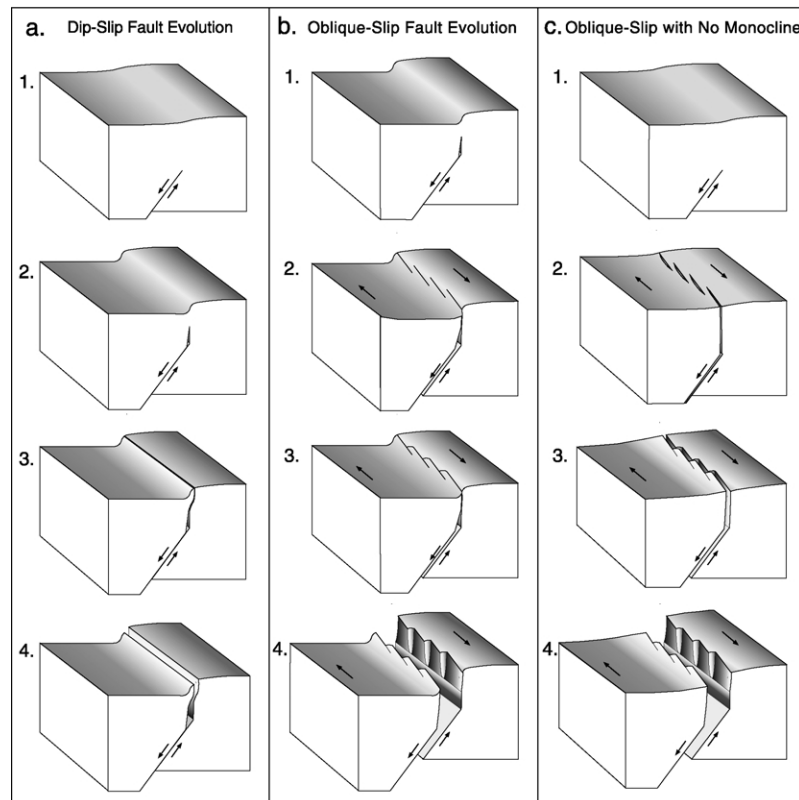


Fig. 15. 3-D block diagrams illustrating conceptual models for normal fault evolution in southwest Iceland. (a) Dip-slip normal faults. (1) A dipping normal fault initiates in the subsurface and propagates upwards. (2) A vertical fracture forms at the upper fault tip and a narrow monocline develops above it at the surface. (3) The joint propagates to the surface, curving slightly towards the footwall so that it breaches the monocline through the upper hinge. (4) Vertical and opening displacements develop and create a vertical fault scarp at the surface. (b) Oblique-slip normal faults. The sequence of events is similar to (a) except that left-stepping échelon fractures form along the upper tip of a vertical fracture in response to right-lateral oblique motion on the subsurface fault. The fractures breach the monocline upper hinge and link together, developing vertical and opening displacements along vertical, segmented fault scarps. (c) Oblique-slip normal faults with no monoclines form in a similar manner to (b) except that the developing vertical échelon fractures connect to the surface instantaneously by utilizing pre-existing joints in the basalt. The hanging wall and footwall can thus pull apart without a monocline forming.

upper tip of the fracture, producing échelon fractures (Pollard et al., 1982). These échelon fractures would then propagate upwards, breaching the surface in the region of increased tension located along the upper hinge of the monocline. Subsequent slip along the fault would cause these échelon segments to accommodate vertical and opening displacements at the surface. Mechanical interaction and linkage of the segments would ultimately form a through-going fault trace.

Where monoclines are absent along échelon fracture zones (e.g. Echelon Gjá in Fig. 6), oblique slip may have occurred on a dipping fault prior to the development of a vertical fracture along its upper tip. If the resultant échelon fractures created above the fault tip instantly formed a connection to the surface along pre-existing cooling fractures in the basalt, the hanging wall and footwall would be decoupled at the surface along the échelon fractures, allowing the two sides of the fault to pull apart without the creation of a monocline. In this scenario, the only surface bending that would occur would be within the relay ramps between the échelon segments. This type of

deformation occurs at Echelon Gjá and in the Grindavík region (Grant, 2002).

In summary, our model advocating upward-propagating normal faults in southwest Iceland is illustrated in Fig. 15. These mechanically-based conceptual models consider the evolution of dip-slip and oblique-slip normal faults with monoclines, as well as normal faults that lack monoclines.

7. Conclusions

We have presented field evidence and numerical models that strongly support the hypothesis that vertical faults in southwest Iceland propagated to the surface from below. This model contradicts an existing model that hypothesizes fault growth from the surface downwards. Our interpretations are based on the reasoning that downward growth models are incompatible with the existence of monoclinical folds flanking fault zones, as well as existence of en échelon fracture segments with individual segments rotated out of the general trend of the fracture zone.

Our numerical models complement previous experimental, kinematic, and numerical models by taking into account the addition of a vertical fracture to the upper tip of subsurface faults. This vertical fracture develops in response to a region of high tensile stress above the upper tip of a slipping normal fault. Our model results show that a vertical fracture attached to a normal fault with its upper tip at a depth of 250–500 m (or 25–50% of the fault length) results in the development of a narrow monoclinical fold above the fracture at the surface. Monocline width decreases as the upper tip of the fracture approaches the surface. Vertical fractures breach the surface through a zone of high tensile surface stress along the upper hinge of the monocline. The limb of the monocline thus occurs on the hanging wall side of the fault trace. These results closely resemble narrow monoclinical folds that flank normal fault traces in southwest Iceland.

Fracture zones containing échelon fault or fracture segments rotated out of the general trend of the fault zone are indicative of oblique-normal slip on an underlying fault. The resultant rotation of the principal stresses above the fault tip produces échelon fracture segments that propagate upwards to the surface. Such fracture patterns are particularly common in oblique spreading areas such as the Reykjanes Peninsula, but only occur along fault bends where spreading is perpendicular to fracture zones, such as at Thingvellir. If oblique slip occurs on a subsurface normal fault containing a vertical fracture at its upper tip, a narrow monocline may exist at the surface, in which case the échelon fractures breach the surface through the monocline upper hinge. If oblique slip occurs on a subsurface fault without a vertical fracture, or if the upper tip of the vertical fracture is several hundreds of meters deep, échelon fractures may breach the surface without concomitant monocline development.

Acknowledgements

This research was funded by a University of Idaho Seed Grant (to Kattenhorn), a graduate research grant (to Grant) from the Geological Society of America, a James Francis Fitzgerald scholarship (to Grant) from the University of Idaho, and a Francis S. Viele scholarship (to Grant) from the Sigma Phi Society. Reviews by Juliet Crider and Valerio Acocella resulted in a much improved revised manuscript. We thank Amy Clifton at the Nordic Volcanological Institute in Reykjavik for guidance and logistical support. Thanks to the people of Iceland for unselfishly sharing their haven with giddy foreign geologists.

References

Acocella, V., Gudmundsson, A., Funicello, R., 2000. Interaction and linkage of extension fractures and normal faults: examples from the rift zone of Iceland. *Journal of Structural Geology* 22, 1233–1246.

- Acocella, V., Korme, T., Salvini, F., 2003. Formation of normal faults along the axial zone of the Ethiopian Rift. *Journal of Structural Geology* 25, 503–513.
- Allmendinger, R.W., 1998. Inverse and forward numerical modeling of trishear fault-propagation folds. *Tectonics* 17, 640–656.
- Angelier, J., Bergerat, F., Dauteuil, O., Villemin, T., 1997. Effective tension-shear relationships in extensional fissure swarms, axial rift zone of Northeastern Iceland. *Journal of Structural Geology* 19, 673–685.
- Cartwright, J.A., Mansfield, C.S., 1998. Lateral displacement variation and lateral tip geometry of normal faults in the Canyonlands National Park, Utah. *Journal of Structural Geology* 20, 3–19.
- Cartwright, J.A., Trudgill, B.D., Mansfield, C.S., 1995. Fault growth by segment linkage: an explanation for scatter in maximum displacement and trace length data from the Canyonlands Grabens of SE Utah. *Journal of Structural Geology* 17, 1319–1326.
- Clark, S.P.J., 1966. *Handbook of Physical Constants*, Geological Society of America, New York, 587pp.
- Clifton, A.E., 2000. Laboratory and field studies of fracture populations produced by oblique rifting. Unpublished Ph.D. thesis, Rutgers University.
- Clifton, A.E., Schlichte, R.W., 2003. Fracture populations on the Reykjanes Peninsula, Iceland: comparison with experimental clay models of oblique rifting. *Journal of Geophysical Research* 108, 2074 doi:10.1029/2001JB000635.
- Clifton, A.E., Schlichte, R.W., Withjack, M.O., Ackermann, R.V., 2000. Influence of rift obliquity on fault-population systematics: results of experimental clay models. *Journal of Structural Geology* 22, 1491–1510.
- Crider, J.G., 2001. Oblique slip and the geometry of normal fault linkage: mechanics and a case study from the Basin and Range in Oregon. *Journal of Structural Geology* 23, 1997–2009.
- Crider, J.G., Pollard, D.D., 1998. Fault linkage: three-dimensional mechanical interaction between échelon normal faults. *Journal of Geophysical Research* 103, 24,373–24,391.
- DeMets, C., Gordon, R., Argus, D., Stein, S., 1994. Effect of recent revisions to the geomagnetic reversal time scale on estimates of current plate motions. *Geophysical Research Letters* 21, 2191–2194.
- dePolo, C.M., Clark, D.G., Slemmons, D.B., Ramelli, A.R., 1991. Historical surface faulting in the Basin and Range province, western North America: implications for fault segmentation. *Journal of Structural Geology* 13, 123–136.
- Einarsson, T., 1967. The Icelandic fracture system and the inferred causal stress field. In: Björnsson, S. (Ed.), *Iceland and Mid-Ocean Ridges*. *Societate Scientiarum Islandica* 38, pp. 128–139.
- Einarsson, P., 1991. Earthquakes and present day tectonism in Iceland. *Tectonophysics* 189, 261–279.
- Erslev, E.A., 1991. Trishear fault-propagation folding. *Geology* 19, 617–620.
- Grant, J.V., 2002. Normal fault evolution at an extensional plate boundary, southwest Iceland: a field and numerical modeling investigation. Unpublished M.S. thesis, University of Idaho.
- Gudmundsson, A., 1980. The Vogar fissure swarm, Reykjanes Peninsula, SW Iceland. *Jökull* 30, 43–64.
- Gudmundsson, A., 1987a. Geometry, formation and development of tectonic fractures on the Reykjanes Peninsula, southwest Iceland. *Tectonophysics* 139, 295–308.
- Gudmundsson, A., 1987b. Tectonics of the Thingvellir fissure swarm, SW Iceland. *Journal of Structural Geology* 9, 61–69.
- Gudmundsson, A., 1992. Formation and growth of normal faults at the divergent plate boundary in Iceland. *Terra Nova* 4, 464–471.
- Gudmundsson, A., Bäckström, K., 1991. Structure and development of the Sveinagja graben, Northeast Iceland. *Tectonophysics* 200, 111–125.
- Haimson, B.C., 1979. New stress measurements in Iceland reinforce previous hydrofracturing results. *Eos, Transactions of the American Geophysical Union* 60, 377.
- Haimson, B.C., Rummel, F., 1982. Hydrofracturing stress measurements in the Iceland research drilling project drill hole at Reydarfjörður, Iceland. *Journal of Geophysical Research* 87, 6631–6649.
- Johannesson, H., Saemundsson, K., 1989. *Geological Map of Iceland*.

- Icelandic Museum of Natural History and Icelandic Geodetic Survey, Reykjavik, 1:500,000.
- Kattenhorn, S.A., Pollard, D.D., 1999. Is lithostatic loading important for the slip behavior and evolution of normal faults in the Earth's crust? *Journal of Geophysical Research* 104, 28,879–28,898.
- Kattenhorn, S.A., Pollard, D.D., 2001. Integrating 3-D seismic data, field analogs, and mechanical models in the analysis of segmented normal faults in the Wytch Farm oil field, southern England, United Kingdom. *American Association of Petroleum Geologists Bulletin* 85, 1183–1210.
- Kattenhorn, S.A., Aydin, A., Pollard, D.D., 2000. Joints at high angles to normal fault-strike: an explanation using 3-D numerical models of fault-perturbed stress fields. *Journal of Structural Geology* 22, 1–23.
- Landmælingar Íslands, 1994. Thingvellir. Icelandic Geodetic Survey, Akranes, Iceland, 1:25,000.
- Langley, J.S., Martel, S.J., 2000. Propagation of normal faults to the surface in basalt. *Eos, Transactions of the American Geophysical Union* 81, F1121.
- Machette, M.N., Personius, S.F., Nelson, A.R., Schwartz, D.P., Lund, W.R., 1991. The Wasatch fault zone, Utah—segmentation and history of Holocene earthquakes. *Journal of Structural Geology* 13, 137–149.
- Maerten, L., 2000. Variation in slip on intersecting normal faults; implications for paleostress inversion. *Journal of Geophysical Research* 105, 25,553–25,565.
- Maerten, L., Pollard, D.D., Karpuz, R., 2000. How to constrain 3-D fault continuity and linkage using reflection seismic data. *American Association of Petroleum Geologists Bulletin* 84, 1311–1324.
- Maerten, L., Gillespie, P., Pollard, D.D., 2002. Effects of local stress perturbation on secondary fault development. *Journal of Structural Geology* 24, 145–153.
- Mansfield, C.S., Cartwright, J.A., 1996. High resolution fault displacement mapping from three-dimensional seismic data: evidence for dip linkage during fault growth. *Journal of Structural Geology* 18, 249–263.
- Martel, S.J., 1997. Effects of cohesive zones on small faults and implications for secondary fracturing and fault trace geometry. *Journal of Structural Geology* 19, 835–847.
- McGill, G.E., Stromquist, A.W., 1975. Origin of grabens in the Needles district, Canyonlands National Park, Utah. *Four Corners Geological Society, Durango, CO*, 235–243.
- McGill, G.E., Stromquist, A.W., 1979. The grabens of Canyonlands National Park, Utah: geometry, mechanics, and kinematics. *Journal of Geophysical Research* 84, 4547–4563.
- Muffler, P., Clynne, M., Champion, D., 1994. Late Quaternary normal faulting of the Hat Creek Basalt, northern California. *Bulletin of the Geological Society of America* 106, 195–200.
- Nakamura, K., 1970. En échelon features of Icelandic ground fissures. *Acta Naturalia Islandica* 2, 3–15.
- Nicol, A., Watterson, J., Walsh, J.J., Childs, C., 1996. The shapes, major axis orientations and displacement patterns of fault surfaces. *Journal of Structural Geology* 18, 235–248.
- Opheim, J., Gudmundsson, A., 1989. Formation and geometry of fractures, and related volcanism, of the Krafla fissure swarm, Northeast Iceland. *Bulletin of the Geological Society of America* 101, 1608–1622.
- Patton, T.L., Fletcher, R.C., 1995. Mathematical block-motion model for deformation of a layer above a buried fault of arbitrary dip and sense of slip. *Journal of Structural Geology* 17, 1455–1472.
- Peacock, D.C.P., Parfitt, E.A., 2002. Active relay ramps and normal fault propagation on Kilauea Volcano, Hawaii. *Journal of Structural Geology* 24, 729–742.
- Pollard, D.D., Aydin, A., 1988. Progress in understanding jointing over the past century. *Geological Society of America Bulletin* 100, 1181–1204.
- Pollard, D.D., Segall, P., Delaney, P.T., 1982. Formation and interpretation of dilatant échelon cracks. *Bulletin of the Geological Society of America* 93, 1291–1303.
- Renshaw, C.E., Pollard, D.D., 1994. Numerical simulation of fracture set formation: a fracture mechanics model consistent with experimental observations. *Journal of Geophysical Research* 99, 9359–9372.
- Saemundsson, K., Einarsson, S., 1980. Geological Map of Iceland: SW-Iceland, Sheet 3, 2nd edition, Museum of Natural History and the Icelandic Geodetic Survey, Reykjavik, 1:250,000.
- Schlische, R.W., Withjack, M.O., Eisenstadt, G., 2002. An experimental study of the secondary deformation produced by oblique-slip normal faulting. *American Association of Petroleum Geologists Bulletin* 86, 885–906.
- Stock, J.M., Healy, J.H., Hickman, S.H., Zoback, M.D., 1985. Hydraulic fracturing stress measurements at Yucca Mountain, Nevada, and relationship to the regional stress field. *Journal of Geophysical Research* 90, 8691–8706.
- Stromquist, A., 1976. Geometry and growth of grabens, Lower Red Lake Canyon area, Canyonlands National Park, Utah. Contribution No. 28, Department of Geology and Geography, University of Massachusetts, Amherst, 118pp.
- Taylor, B., Crook, K., Sinton, J., 1994. Extensional transform zones and oblique spreading centers. *Journal of Geophysical Research* 99, 19, 707–19,718.
- Thomas, A.L., 1993. Poly3D: a three dimensional, polygonal element, displacement discontinuity boundary element computer program with applications to fractures, faults, and cavities in the Earth's crust. Unpublished M.S. thesis, Stanford University.
- Trudgill, B., Cartwright, J., 1994. Relay-ramp forms and normal-fault linkages, Canyonlands National Park, Utah. *Bulletin of the Geological Society of America* 106, 1143–1157.
- Vadon, H., Sigmundsson, F., 1997. Crustal deformation from 1992 to 1995 at the Mid-Atlantic Ridge, Southwest Iceland, mapped by satellite radar interferometry. *Science* 275, 193–197.
- Walsh, J.J., Watterson, J., 1989. Displacement gradients on fault surfaces. *Journal of Structural Geology* 11, 307–316.
- Willemse, E.J.M., 1997. Segmented normal faults: correspondence between three-dimensional mechanical models and field data. *Journal of Geophysical Research* 102, 675–692.
- Willemse, E.J.M., Pollard, D.D., Aydin, A., 1996. Three-dimensional analyses of slip distributions on normal fault arrays with consequences for fault scaling. *Journal of Structural Geology* 18, 295–309.
- Williams, R.S., 1995. Icelandic–English Glossary of Selected Geoscience Terms. United States Geological Survey.
- Willsey, S.P., Umhoefer, P.J., Hilley, G.E., 2002. Early evolution of an extensional monocline by a propagating normal fault: 3D analysis from combined field study and numerical modeling. *Journal of Structural Geology* 24, 651–669.
- Withjack, M.O., Olson, J., Peterson, E., 1990. Experimental models of extensional forced folds. *American Association of Petroleum Geologists Bulletin* 74, 1038–1054.
- Wu, H., Pollard, D.D., 1992. Propagation of a set of opening-mode fractures in layered brittle materials under uniaxial strain cycling. *Journal of Geophysical Research* 97, 3381–3396.
- Wu, H., Pollard, D.D., 1995. An experimental study of the relationship between joint spacing and layer thickness. *Journal of Structural Geology* 17, 887–905.
- Zhang, P., Slemmons, D.B., Mao, F., 1991. Geometric pattern, rupture termination and fault segmentation of the Dixie Valley–Pleasant Valley active normal fault system, Nevada, USA. *Journal of Structural Geology* 13, 165–176.
- Zoback, M.D., Healy, J.H., 1984. Friction, faulting, and in situ stress. *Annales Geophysicae* 2, 689–698.